Biomedicine & Pharmacotherapy 144 (2021) 112310

Contents lists available at ScienceDirect

Biomedicine & Pharmacotherapy

journal homepage: www.elsevier.com/locate/biopha

Zebrafish as a model to study inflammation: A tool for drug discovery

Marco A.A. Belo [a,b], Melque F. Oliveira [a], Susana L. Oliveira [b], Mayumi F. Aracati [b], Letícia F. Rodrigues [b], Camila C. Costa [b], Gabriel Conde [b], Juliana M.M. Gomes [c], Mariana N. L. Prata [d], Ayslan Barra [d], Thalita M. Valverde [c,e], Daniela C. de Melo [f], Silas F. Eto [g], Dayanne C. Fernandes [h], Marina G.M.C. Romero [d], José D. Corrêa Júnior [c], Juliana O. Silva [i], Andre L.B. Barros [i], Andrea C. Perez [d], Ives Charlie-Silva [j,*]

[a] Laboratory of Animal Pharmacology and Toxicology, Brazil University (UB), Descalvado, Brazil
[b] Department of Preventive Veterinary Medicine, São Paulo State University (UNESP), Jaboticabal, Brazil
[c] Department of Morphology, Federal University of Minas Gerais (UFMG), Belo Horizonte, Brazil
[d] Department of Physiology and Pharmacology, Federal University of Minas Gerais (UFMG), Belo Horizonte, Brazil
[e] Department of Biochemistry and Immunology, Federal University of Minas Gerais (UFMG), Belo Horizonte, Brazil
[f] Department of zootechnics at the Veterinary School, Federal University of Minas Gerais (UFMG), Belo Horizonte, Brazil
[g] Postgraduate Program in Health Sciences - PROCISA, Federal University of Roraima, Brazil
[h] Immunochemistry Laboratory, Butantan Institute, São Paulo, Brazil
[i] Department of Clinical and Toxicological Analyses, Federal University of Minas Gerais (UFMG), Belo Horizonte, Brazil
[j] Department of Pharmacology, University of São Paulo (ICB-USP), São Paulo, Brazil

ARTICLE INFO

Keywords:
Inflammatory reaction
Teleost fish
Innate Immunity
Acute and chronic inflammation
Foreign body reaction
Xenotransplantation

ABSTRACT

This study aims to demonstrate the applicability and importance of zebrafish (*Danio rerio*) model to study acute and chronic inflammatory responses induced by different stimuli: carrageenan phlogogen (nonimmune); acute infection by bacteria (*immune)*; foreign body reaction (chronic inflammation by round glass coverslip implantation); reaction induced by xenotransplantation. In addition to the advantages of presenting low breeding cost, high prolificity, transparent embryos, high number of individuals belonging to the same spawning and high genetic similarity that favor translational responses to vertebrate organisms like humans, zebrafish proved to be an excellent tool, allowing the evaluation of edema formation, accumulation of inflammatory cells in the exudate, mediators, signaling pathways, gene expression and production of specific proteins. Our studies demonstrated the versatility of fish models to investigate the inflammatory response and its pathophysiology, essential for the successful development of studies to discover innovative pharmacological strategies.

1. Introduction

Inflammation is an essential body defense mechanism involved in tissue restoration. This mechanism is composed of signaling molecules, defense, and repair cells, with the objective of restoring the physiological balance, being an essential response for the body [1]. Although it is a defense mechanism, the inflammatory response, when excessive, prolonged, and uncontrolled, causes tissue damage and contributes to the pathogenesis of acute and chronic inflammatory diseases such as rheumatoid arthritis, multiple sclerosis, systemic lupus erythematosus and stroke [2].

Advances in research in the medical field depend on studies involving experimental animal models, and about 95% of the studies carried out involve the use of mice and rats. Animal models are widely used to understand the pathophysiological mechanisms in the inflammatory process, the agents involved in diseases associated with inflammation and, therefore, to investigate new drugs and therapies [3]. In this context, the zebrafish (*Danio rerio*) has demonstrated several advantages over other species and may be an alternative to the use of rodents or provide additional information when used as a model for studies of inflammatory diseases [4–7], pharmacological and toxicological studies [8–12] and even the study of new drugs [13,14].

Among the advantages of using zebrafish for the development of drugs, it is worth highlighting the reproductive capacity of these animals

* Correspondence to: Department of Pharmacology, University of São Paulo (ICB-USP), Professor Lineu Prestes 1524 Prédio ICB 1 - Butantã, São Paulo 05508-000, Brazil.
E-mail address: charliesilva4@hotmail.com (I. Charlie-Silva).

https://doi.org/10.1016/j.biopha.2021.112310
Received 24 August 2021; Received in revised form 20 September 2021; Accepted 5 October 2021
Available online 19 October 2021

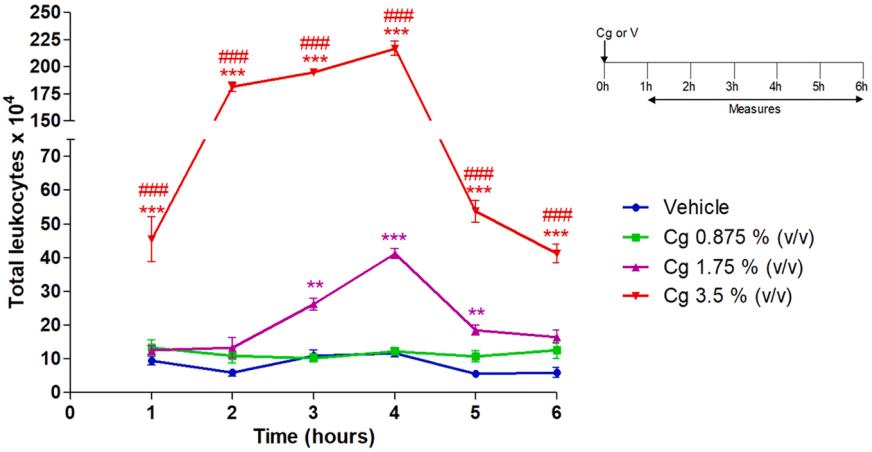

Fig. 1. Time curve of the phlogogenic effect induced by intracoelomatic injection of different concentrations of carrageenan (Cg), on the total number of leukocytes. Each symbol represents the mean ± S.E.M. of the number of leukocytes counted in Neubauer's chamber. * * $p < 0.01$ compared to the control group, * ** $p < 0.001$ compared to the control group (vehicle, sterile saline solution); ### $p < 0.001$ compared to the Cg treatment 1.75% (v / v).

resulting in a high number of individuals belonging to the same spawning, transparent embryos, low cost of breeding and high genetic similarity that favor translational responses to vertebrate organisms like humans [15]. Zebrafish genome has been completely sequenced, sharing high similarity with the human genome [16]. Recently, Forn-Cuní et al. [5] demonstrated that the zebrafish inflammatory response can effectively reproduce the inflammatory process in a mammal. In addition, the authors provided evidence that immune signaling pathways and gene expression are well conserved throughout evolution. In research, just like any animal, it is necessary to first understand its biology, physiology and how the organism responds to pathological induction. Therefore, a study on inflammation or on any subject postulates the standardization of an animal model with controlled and reproducible parameters [17]. For the induction of inflammation in rodents, the administration of carrageenan (Cg) is commonly used. Several animal studies have shown that exposure to Cg causes inflammation, characterized by increased vascular permeability, which leads to extravasation of plasma fluids and migration of leukocytes to the inflammatory focus [18,19].

Classic experimental models in mammals have been used for decades to study the evolution of the inflammatory response in both acute and chronic phases. Some of these protocols have been successfully adapted in fish and have served as an important way to assess the response of teleosts during the evolution of the inflammatory reaction [20]. Among them, there is the aerocystitis model, which mimics the pleurisy technique in rodents, proving to be extremely effective for the study of acute inflammation, as the swim bladder is a cavity organ, delimited, with terminal circulation, easily accessible for inoculation of phlogogens and collection of exudates to assess cellular components and fluids accumulated in the inflammatory focus, in addition to not having resident leukocytes [21,22]. Another important model is the implantation of glass coverslips in the coelomic cavity of fish, which induces a foreign body-type chronic inflammatory response, resulting in the accumulation of macrophages and the formation of multinucleated cells, called giant cells [23,24].

Based on the importance of establishing new experimental models and on the advantages of using zebrafish, associated with the experience of our research group with the use of fish as biomodels, this study aims to demonstrate the applicability and importance of this tool to study acute and chronic inflammatory responses induced by different stimuli: carrageenan phlogogen (nonimmune); acute inflammatory reaction through aerocystitis induced by bacteria (*Aeromonas hydrophila)*; foreign body reaction (chronic inflammation by glass coverslip

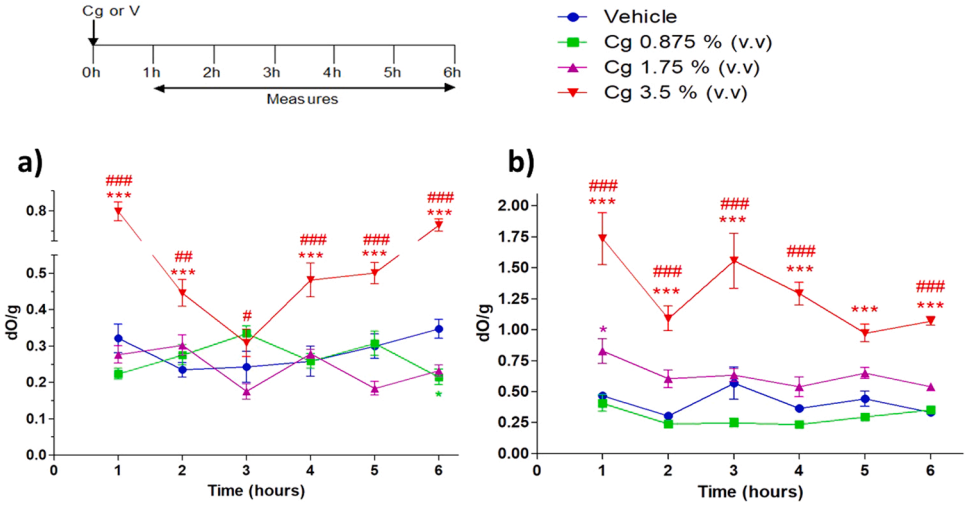

Fig. 2. a) Time curve of the phlogogenic effect induced by the intracoelomatic injection of different concentrations of carrageenan (Cg) on the enzymatic activity of n-acetyl-β-D-glucosaminidase (NAG). Each symbol represents the mean ± S.E.M. of NAG enzymatic activity measured by optical density on weight in grams (dO / g). * $P < 0.05$ compared to the control group (vehicle, sterile saline solution); * ** $p < 0.001$ relative to the control group (vehicle, sterile saline); # $p < 0.05$ relative to the Cg group 1.75% (v / v). ### $p < 0.001$ compared to treatment with Cg 1.75% (v / v). **b)** Time curve of the phlogogenic effect induced by the intracoelomatic injection of different concentrations of carrageenan (Cg) on the enzymatic activity of myeloperoxidase (MPO). Each symbol represents the mean ± S.E.M. of the MPO enzymatic activity measured by optical density on weight in grams (dO / g). * $p < 0.05$ compared to the control group (vehicle, sterile saline); * ** $p < 0.001$ relative to the control group (vehicle, sterile saline); ### $p < 0.001$ compared to treatment with Cg 1.75% (v / v).

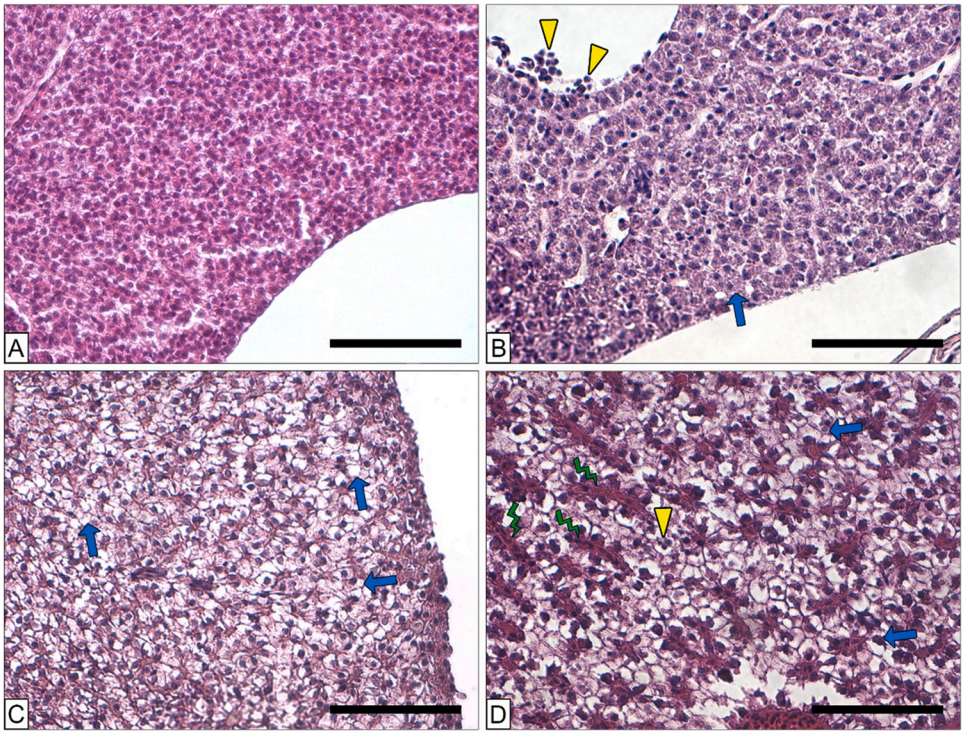

Fig. 3. Histological sections of liver injected with saline (control; A) and carrageenan at concentrations: 0.875% (B), 1.75% and (C) and 3.5% (D). In A the liver is observed with eosinophilic cells, with central nuclei, under physiological conditions. From B to D cells are observed to be numb and vacuolated, with some nuclei displaced to the periphery. In B, mononuclear cells are seen inside the blood vessel. In B and D mononucleated cells are observed in the tissues. Caption: blue arrow: cellular numbness followed by nuclear dislocation to the periphery; yellow arrowhead: tissue leucocytes infiltrates; green ray: hypermyosia of sinusoidal vessels. Sections stained with hematoxylin-eosin. Objectives of 40 x; projective 2 x. Bar = 80 μm.

implantation); inflammatory response induced by xenotransplantation.

2. Results

2.1. Experiment I. Inflammation induced by Carrageenan (Cg)

In this study, we injected carrageenan as a phlogogenic agent in the coelomic cavity and the exudate was evaluated. It was observed that in the concentrations of 3.5% and 1.75% there was a significant increase in the number of total leukocytes compared to the control group. At the concentration of 3.5% there was an extremely significant increase ($p < 0.001$) at all times compared to the control. The concentration of 1.75% brought a significant increase at 3, 4 and 5 h after administration and the concentration of 0.875% did not demonstrate a significant leukocyte recruitment when compared to the control group. There was a difference between the concentrations of 1.75% and 3.5% at all times, and the concentration of 3.5% was able to induce a greater accumulation of leukocytes in the coelomic cavity (Fig. 1). It is also possible to notice that there was a peak of the inflammatory effect within 4 h after administration.

In order to analyze the macrophage infiltrate, the activity of the NAG enzyme (N-Acetylglicosaminidase) (Fig. 2a) was evaluated. It was observed that the curves obtained with Cg at the different concentrations did not present a similar profile among themselves. At the 3.5% concentration, NAG activity is greatly increased at 1, 2, 4, 5 and 6 h after stimulation compared to the group receiving vehicle. It is possible to notice that there was a peak of NAG dosage 1 h after its administration, decreasing subsequently until the third hour, and increasing soon thereafter. There were no differences in the treatments with Cg 0.875% and Cg 1.75% in any of the times compared to the group that received vehicle. There was a significant difference between treatments of 1.75% and 3.5% at all times, and the concentration of 3.5% was able to induce a greater activity of NAG.

Next, the activity of the MPO enzyme (Myeloperoxidase) was evaluated to verify the neutrophil infiltrate (Fig. 2b). It was observed that the curves presented a similar profile over time. The results show that the MPO activity of the treatment that received 3.5% Cg is significantly

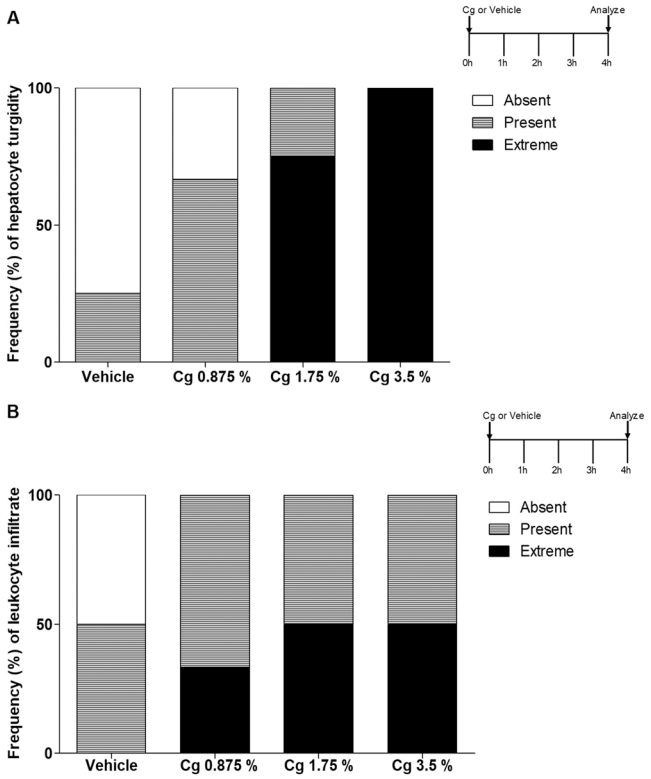

Fig. 4. Liver morphometric data 4 h after intracoelomatic injection of different concentrations of carrageenan (Cg). The frequency of hepatocyte numbness (A) and the frequency of leukocyte infiltrate (B) were qualitatively evaluated.

increased at all times compared to the vehicle receiving group, with a peak of MPO activity 1 h after its administration, decreasing in the second hour, increasing again in the third hour, and reducing soon thereafter. No difference was observed in the treatment of 0.875% over

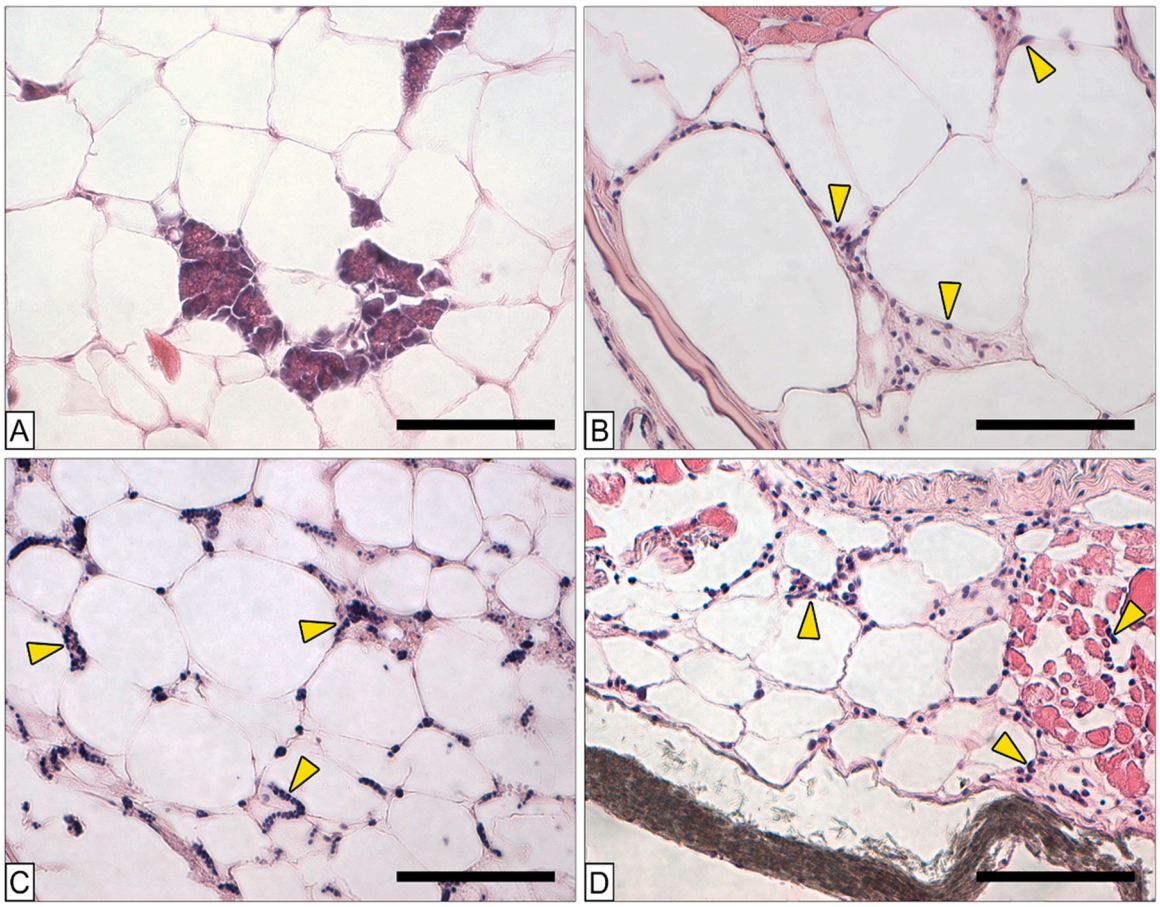

Fig. 5. Histological sections of mesentery injected with saline (control; A) and carrageenan at concentrations: 0.875% (B), Cg 1.75% and (C) and Cg 3.5% (D). In A it is observed mesentery with adipose cells and normal pancreatic tissue, absent of mononuclear cells in the conjunctive part. From B to D, leukocyte infiltrates are observed. In D there are numerous leukocyte infiltrates in the adjacent musculature. Caption: yellow arrowhead: leukocyte infiltrates in the tissues, either in the muscle or between the adipocytes in the connective portion. Sections stained with hematoxylin-eosin. Objectives of 40 x; projective 2 x. Bar = 80 μm.

time compared to the group that received vehicle, but there was an increase in the first hour with the concentration of 1.75%. Except for the fifth hour, there was a significant difference between the concentrations of 1.75% and 3.5% at all times, with the concentration of 3.5% inducing a higher MPO activity.

In order to evaluate microleaks in the organs, once the experiments with the Neubauer chamber identified the leukocyte peak in the fourth hour post stimulus, histological slides of 4 animals were performed for histological and morphometric analysis of the liver, intestine and mesentery at this peak time.

We observed the characteristic of the hepatic parenchyma in organisms injected with vehicle, and with Cg in the concentrations of 0.875%, 1.75% and 3.5% (Fig. 3). The livers of animals injected with the vehicle alone had hepatocytes presenting polygonal shape with

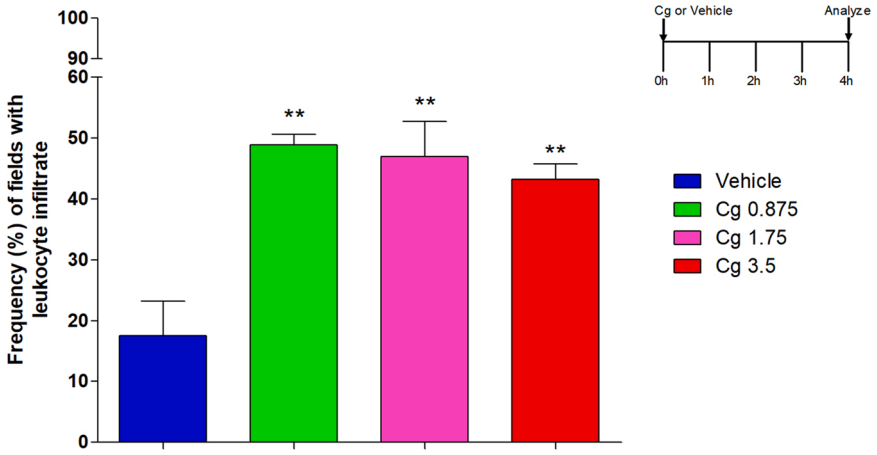

Fig. 6. Morphometric data of the mesentery 4 h after intracoelomatic injection of different concentrations of carrageenan (Cg). The frequency of fields with leukocyte infiltrate were morphometrically evaluated. Each symbol represents the mean ± S.E.M. of the observed frequency. * * $p < 0.01$ relative to the control group (vehicle, sterile saline).

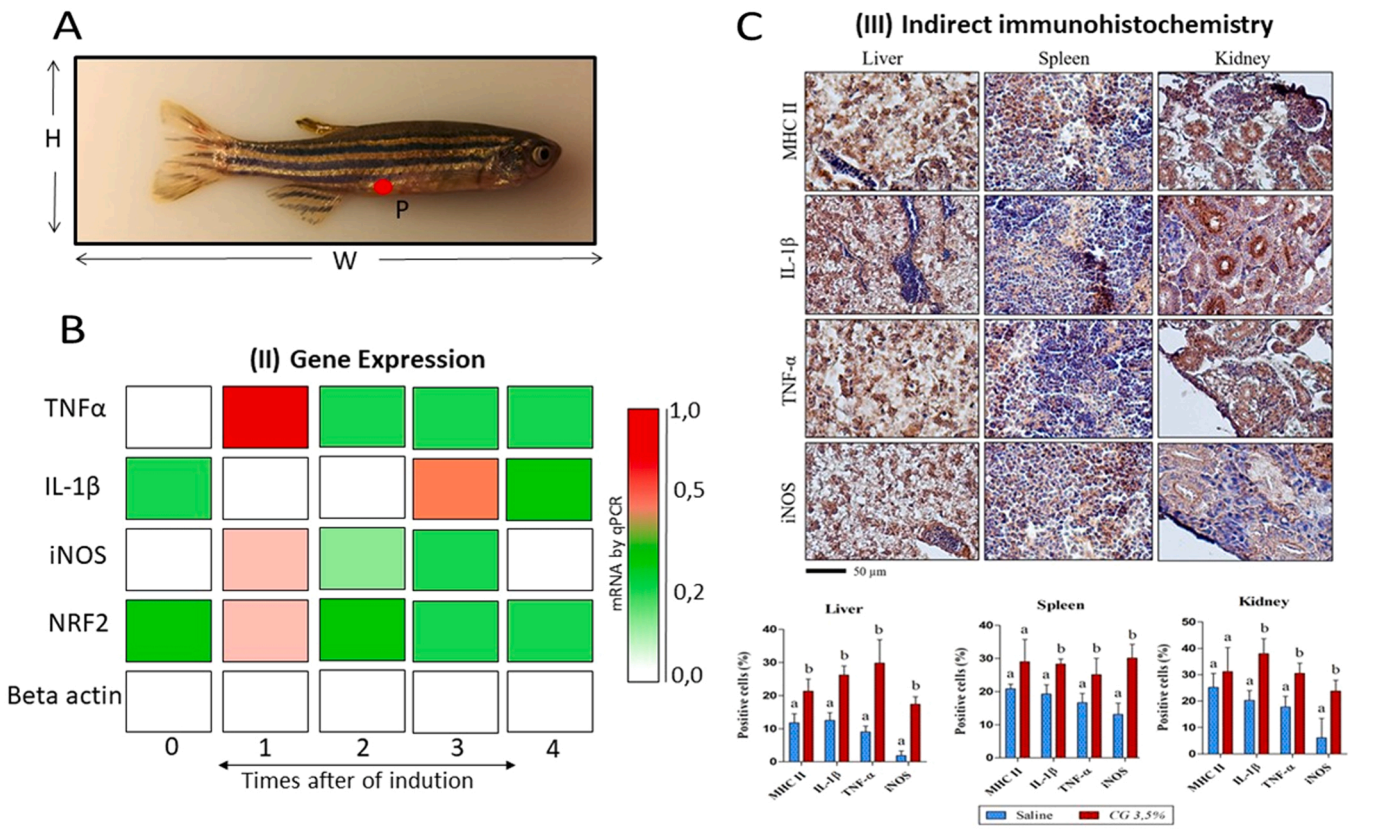

Fig. 7. Kinetics of immune response in carrageenan 3,5% (CG) stimulated zebrafish (*Danio rerio*) tissues and gene expression. (A) carrageenan injection site. (B) Representative images of fish expression gene of NRF2, Interleukin 1β (IL-1β), Tumor necrosis factor α (TNF-α) and nitric oxide synthase (iNOS) times after of induction. (C) Representative images of fish tissues stimulated after 4 h with 3.5% GC and MHC class II positive immune stained (MHC II), Interleukin 1β (IL-1β), Tumor necrosis factor α (TNF-α) and nitric oxide synthase (iNOS) and morphometric analysis of immunoblotted positive cells with the aforementioned markers. Staining: Brown: DAB (3,3-diaminobenzidine) and Harris Hematoxylin. Bar 50 µm.

intensely eosinophilic cytoplasm and purplish, spherical, and central nucleus (Fig. 3A). It was observed a low frequency (or absence) of numbness and minimal presence of leukocyte infiltrates (Fig. 3 B, C and D). These findings are similar to those described by Goessling & Sadler (2015) in normal zebrafish and described by Honorato et al., 2014 for other teleosteal fishes.

In animals injected with Cg, it is noticed that as the concentration increases, the frequency of hepatocytes with a characteristic cytoplasmic vacuolation is increased, followed by numbness (Fig. 4A). There is a decrease in eosinophilia observed in animals treated with Cg at concentrations of 1.75% and 3.5%. The nuclei presented displacement to the periphery mainly in the concentrations of 1.75% and 3.5% (Fig. 3C and D). At the concentration of 0.875%, there is an infiltrate of mononuclear cells near the vascular endothelium. By the morphometry performed, an index of extreme leukocyte infiltrates was observed in half of the animals treated with Cg at concentrations of 1.75% and 3.5% and in one third of the animals treated with Cg at concentrations of 0.875% (Fig. 4B). At the concentration of 3.5%, there is obliteration of the sinusoidal blood vessels present in the liver (Fig. 3D).

The mesentery present in the coelomic cavity of the vehicle receiving group showed connective tissue rich in adipose cells and dispersed pancreatic acini clusters (Fig. 5A) and low frequency of infiltrated leucocyte cells observed (Fig. 6). All these characteristics are in accordance with the literature described in physiological conditions for zebrafish

Table 1
Mean values and ANOVA[1] Total and diferential leucocytes counts of *Danio rerio* challenged by *Aeromonas hydrophila* in different times.

Period	Leukocytes	Thrombocytes	Lymphocytes			Neutrophils			Monocytes	
(HPI) [2]	10^3 /µL	10^3 /µL	R[4]	A[4]		R	A		R	A
6	14.05^{B}	45.44 ^{A}	47.55 ^{C}	7160^{B}		45.55 ^{A}	5874.44 ^{A}		6.88 ^{A}	1021.11^{AB}
12	53.62 ^{A}	35.17^{AB}	83.50^{AB}	37229^{AB}		13.83^{BC}	8361.60 ^{A}		2.66^{B}	1276.66 ^{AB}
18	9.38^{B}	19.38^{B}	71.00^{B}	5620^{B}		26.66^{B}	3586.66^{A}		2.33^{B}	182.22^{B}
24	71.73 ^{A}	46.11 ^{A}	85.85^{AB}	44582 ^{A}		12.14^{BC}	7447.00 ^{A}		2.00^{B}	1387.71 ^{A}
36	54.69 ^{A}	51.19 ^{A}	88.63 ^{A}	47507 ^{A}		9.54 ^{C}	6377.63 ^{A}		1.81^{B}	812.63^{AB}
48	49.68 ^{A}	52.79 ^{A}	88.09 ^{A}	43983 ^{A}		8.27 ^{C}	4122.90 ^{A}		3.63^{B}	1580.63 ^{A}
F value	5.61	2.30	9.21	7.20		7.58	0.45		2.53	1.79
Pr > F[3]	0.0004	0.0586	< .0001	< .0001		< .0001	0.8111		0.0414	0.1339
110.57	110.58	110.59	110.60	110.61	110.62	110.63	110.64	110.65	110.66	110.67

[1]Means (n = 10) followed by the same letters in the column do not differ by the *t*-test ($p < 0.05$).
[2] HPI = Hours post-infection.
[3] Pr>F: probability of significance of F; CV: Coefficient of variation.
[4]R- Relative percentage values; A – Absolute cell counts.

Table 2
Mean values and ANOVA[1] Total and differential counts of inflammatory cells present in the swim bladder of *Danio rerio* challenged by *Aeromonas hydrophila* in different times.

Period	Total	Lymphocytes		Granulocytes		Macrophages		Thrombocytes	
(HPI) [2]	Cells	R[4]	A[4]	R	A	R	A	R	A
6	29318.18^{B}	37.62^{AB}	11023.63^{B}	30.98^{B}	9076.90^{B}	14.70^{B}	4309.77^{B}	16.74 ^{A}	4907.86^{AB}
12	78333.33^{AB}	29.16^{B}	22841.99^{B}	33.33^{B}	26108.49^{B}	35.83 ^{A}	28066.83 ^{A}	1.66^{B}	1300.33^{B}
18	128727.27 ^{A}	40.04^{AB}	51542.39 ^{A}	47.66^{AB}	61351.41 ^{A}	6.87^{B}	8843.56^{B}	5.40^{B}	6951.27 ^{A}
24	17045.40^{B}	37.45^{AB}	6383.50^{B}	53.00 ^{A}	9034.06^{B}	5.45^{B}	928.97^{B}	4.09^{B}	697.15^{B}
36	24363.62^{B}	48.45 ^{A}	11804.17^{B}	41.18^{AB}	10032.93^{B}	7.27^{B}	1771.23^{B}	3.09^{B}	752.83^{B}
48	29000.08^{B}	51.70 ^{A}	14993.04^{B}	31.70^{B}	9193.02^{B}	14.70^{B}	4263.01^{B}	1.90^{B}	551.00^{B}
F value	7.39	1.91	11.70	3.50	6.59	6.89	2.82	7.20	3.51
Pr > F[3]	< .0001	0.1082	< .0001	0.0082	< .0001	< .0001	0.0245	< .0001	0.0080
C. V.[3]	162.88	40.61	134.92	39.19	195.86	93.39	430.27	116.22	245.47

[1] Means (n = 10) followed by the same letters in the column do not differ by the *t*-test ($p < 0.05$).
[2] HPI = Hours post-infection.
[3] Pr>F: probability of significance of F; CV: Coefficient of variation.
[4]R- Relative percentage values; A – Absolute cell counts.

Mononuclear cells were observed in the conjunctival portion at higher frequency in Cg treated animals (Fig. 5 B, C, D and Fig. 6). At the concentration of 3.5% (Fig. 5 D), cellular infiltrate can also be seen in the adjacent muscle.

Then, the expression of the inflammatory genes induced by carrageenan was investigated in a zebrafish model with a concentration of 3.5% (Fig. 7B). Tumor necrosis factor-α, (TNF-α) mRNA expression at the injection site increased 1 h after carrageenan inoculation and slowly decreased over the subsequent hours. However, it was still detected after 4 h (Fig. 7B). In addition, nuclear factor 2 related to erythroid factor 2 (NRF2) and inducible nitric oxide synthase mRNA (iNOS) showed moderate expression 1 h after challenge (Fig. 7B). On the other hand, the expression of the interleukin 1-beta (IL-1β) gene had a transient reduction in the first two hours, and after the third hour of challenge, there was a significant expression of mRNA. To confirm the gene expression data, liver, spleen, and kidney were evaluated for the expression of TNF-α, IL-1β, iNOS and MHC II proteins. Corroborating gene expression, injection of 3.5% carrageenan increased the production of IL-1β, TNF-α and iNOS in liver, spleen and kidney (Fig. 7C). In the kidney, renal tubules and vascular endothelium were immunoreactive for IL-1β and iNOS, results already expected due to the physiological production of inflammatory mediators in this area. There was also a significant increase in MHC class II positive cells compared to the control group (Fig. 7B and C).

2.2. Experiment II. Inflammation induced by a bacterial agent

In this assay, we injected a bacterial agent into the swim bladder and evaluated the total and differential leukocyte counts present in the blood and exudate of zebrafish challenged by *Aeromonas hydrophila* at different times. After the challenge we observed a significant decrease ($p < 0.05$) in total leukocyte counts during acute aerocystitis with 6 and 18 h after challenge. However, the lowest counts were observed with 18 h after challenge (Table 1), marked by a significant decrease ($p < 0.05$) in the number of lymphocytes and monocytes.

In *D. rerio* swim bladder exudate, there was a significant increase ($p < 0.05$) in the recruitment of leukocytes over time and macrophages 12 h after challenge, both in relative percentage values and in absolute counts (Table 2). In addition, *D. rerio* exudate showed a significant increase in thrombocytes in relative percentage values ($p < 0.05$) and in absolute counts in the most acute phase with 6 h after challenge. There were no significant variations ($p > 0.05$) in absolute neutrophil counts in all periods observed.

2.3. Experiment III. Foreign body reaction (Chronic inflammation induced by a glass coverslip)

In this study, we implanted a 3 mm round glass coverslip as an inflammatory agent in the coelomic cavity and characterized for the first time in zebrafish the chronic inflammatory response. In this assay, after a coverslip implantation, we evaluated the total white blood cell count present in the blood at different times and inflammatory cells in the glass coverslip.

In the hematological analysis (Fig. 8) no significant erythrocyte and thrombocytic differences were observed between the periods, but in the evaluation of the white blood cell count (Fig. 9) it was possible to see higher values of the total number of leukocytes in the first two periods followed by a fall, with its peak in 48 h; intermittent values of fall in the periods of 72, 96 and 120 h, and elevation in 48 and 96 h of lymphocytes and monocytes and elevated counts of neutrophils in the first period of

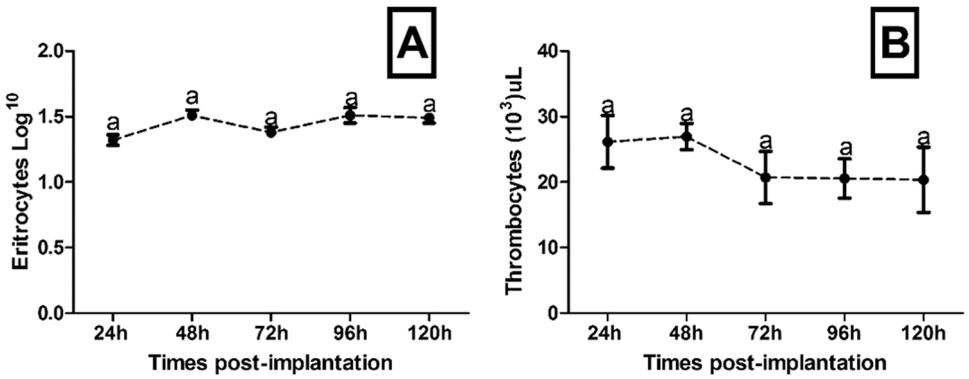

Fig. 8. – Mean values (± S.E.) for total Erythrocytes (A) and Thrombocytic cells (B) in different times. ANOVA is represented in small letters and differente letters show significant difference *t*-test ($p < 0.05$).

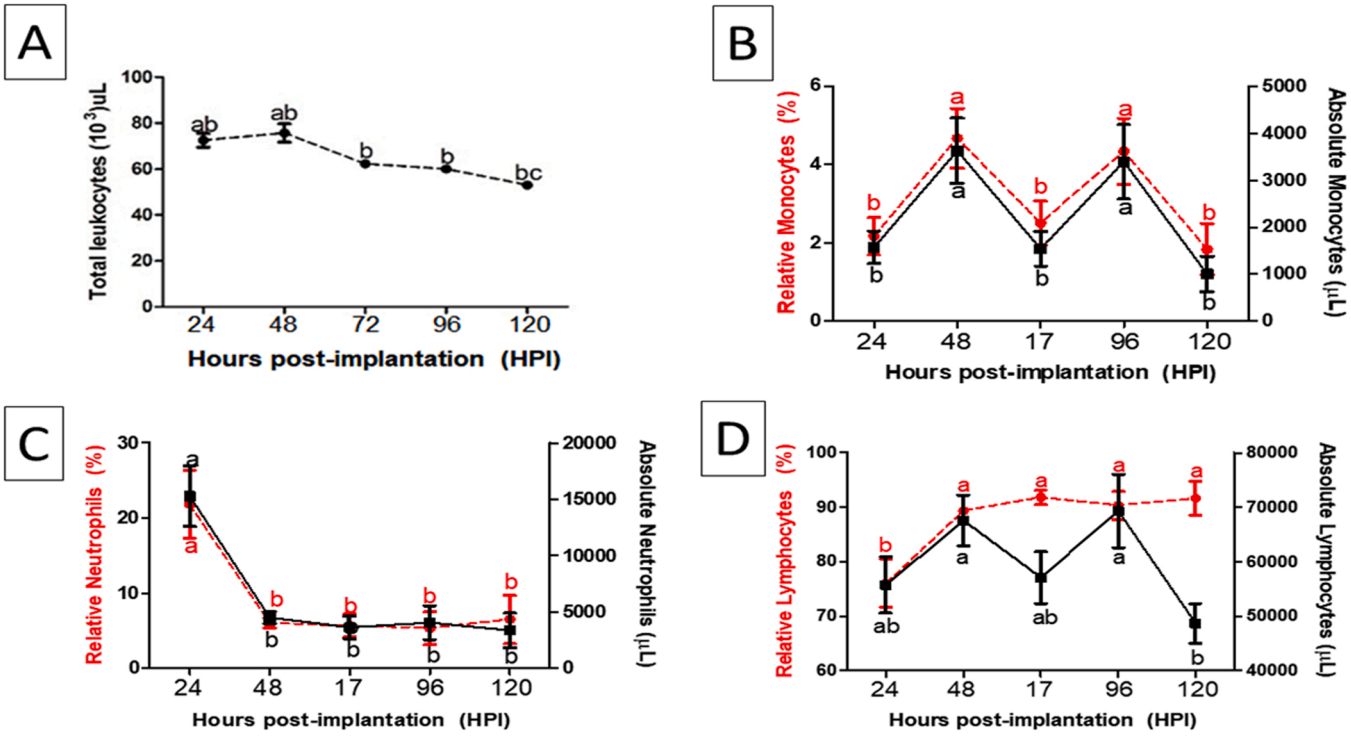

Fig. 9. Mean values (± SD) for total leukocyte counts (A) and relative (red) and absolute (black) differential count of monocytes (B), neutrophils (C) and lymphocytes (D) at different times. The analysis of variance is represented by lowercase letters for comparison between treatments and different letters indicate a significant difference by the *t*-test ($p < 0.05$).

the experiment, preceeded by a fall.

Then, we evaluated the accumulation of macrophages present on the coverslips at different periods. After implantation there was an increase in the accumulation of macrophages over time after implantation, as shown in Fig. 10. Such differences were evidenced, mainly, in the accumulation macrophages (1 nucleus) in the first two periods, followed by a decrease, and with a new increase in the period of 96 h; 3–4 and ≥ 5 nuclei were observed only in periods of 48 and 96 h. Upon analyzing the slides, the formation of a multinucleated giant Langerhans cell (LGC) 96 h after implantation was observed.

2.4. Experiment IV. Inflammation induced by xenotransplant

In this experiment, we performed a xenotransplantation of human breast tumor cells into the zebrafish coelomic cavity and analyzed the inflammatory response and non-invasive tumor development analyzed in 3 times over 21 days (T7 days, T14 days and T21 days). The xenotransplantation assay of tumor cells in adult zebrafish revealed that, regardless of the time evaluated, all animals showed cell fluorescence in the same region where the tumor cells were injected after 14 and 21 days after implant. Over time, measurement of the fluorescence area indicated an increase of tumor proliferation (Figs. 11 and 12). Histological results confirmed the presence of tumor cells in addition to an inflammatory response with tumor capsule formation (Fig. 11). In the liver, melanomacrophagic centers were observed and increased vascularization and pigmentation change around its capsule showing an increased inflammatory infiltrate, demonstrating a response of the immune system (Fig. 11).

3. Discussion

We demonstrated in a series of sequential experiments a model of inflammatory response (acute and chronic) in zebrafish. Therefore, we performed numerous experiments to understand the mediators and cellular responses involved in the acute and chronic inflammatory response. In these studies, the inflammatory response was characterized by the formation of edema in the abdominal region and accumulation of inflammatory cells in the exudate both in the phlogogen model and in the bacterium-induced model, gene expression and production of proteins associated with the inflammatory process. Furthermore, the findings reported here foreign body reaction are pioneering, as we describe a new and useful zebrafish model to investigate the inflammatory response and possible use to study drugs and discover new innovative pharmacological tools.

In the first trial, a peak of leukocyte accumulation in zebrafish occurred after 4 h of Cg 3.5% injection corroborating the findings of [7, 25]. These findings are relevant when considering the search for new substances with anti-inflammatory potential.

Both Cg concentration of 1.75% and 3.5% demonstrated the 4 h peak. This 4 h interval is also observed in rodents. There is an increase in white blood cells, nitric oxide products (nitrites and nitrates), myeloperoxidase, interleukin-1 (IL-1) and local and systemic exsudate [26]. Ekambaram et al. [25] reported an increase in abdominal volume, TNF-α and iNOS and in cellular infiltrate in the abdominal muscle after 4 h of 3.5% Cg injection.

N-Acetylglicosaminidase (NAG) is a hydrophilic lysosomal enzyme responsible for breaking chemical bonds of glycosides that form structural components in many tissues. It is responsible for eliminating cellular waste, including the cell membrane. Its release probably occurs by lysosomal exocytosis [27]. It is produced by macrophages [28], that also release pro-inflammatory interleukins and chemokines, ROS and reactive nitrogen intermediates, such as nitric oxide in the inflammatory process. Its activity is related to a variety of pathologies associated with macrophage-mediated inflammation, such as diabetes, systemic lupus erythematosus, microangiopathies and neoplasms, stomach, liver, breast and pancreas cancer [29]. NAG is commonly measured and is an indicator of damage to the tubular epithelium [29]. Therefore, measuring NAG activity is an indirect indicator of the presence or activation of macrophages in tissue during the inflammatory process [28]. In this study, 3.5% Cg initially increased NAG activity in the first two

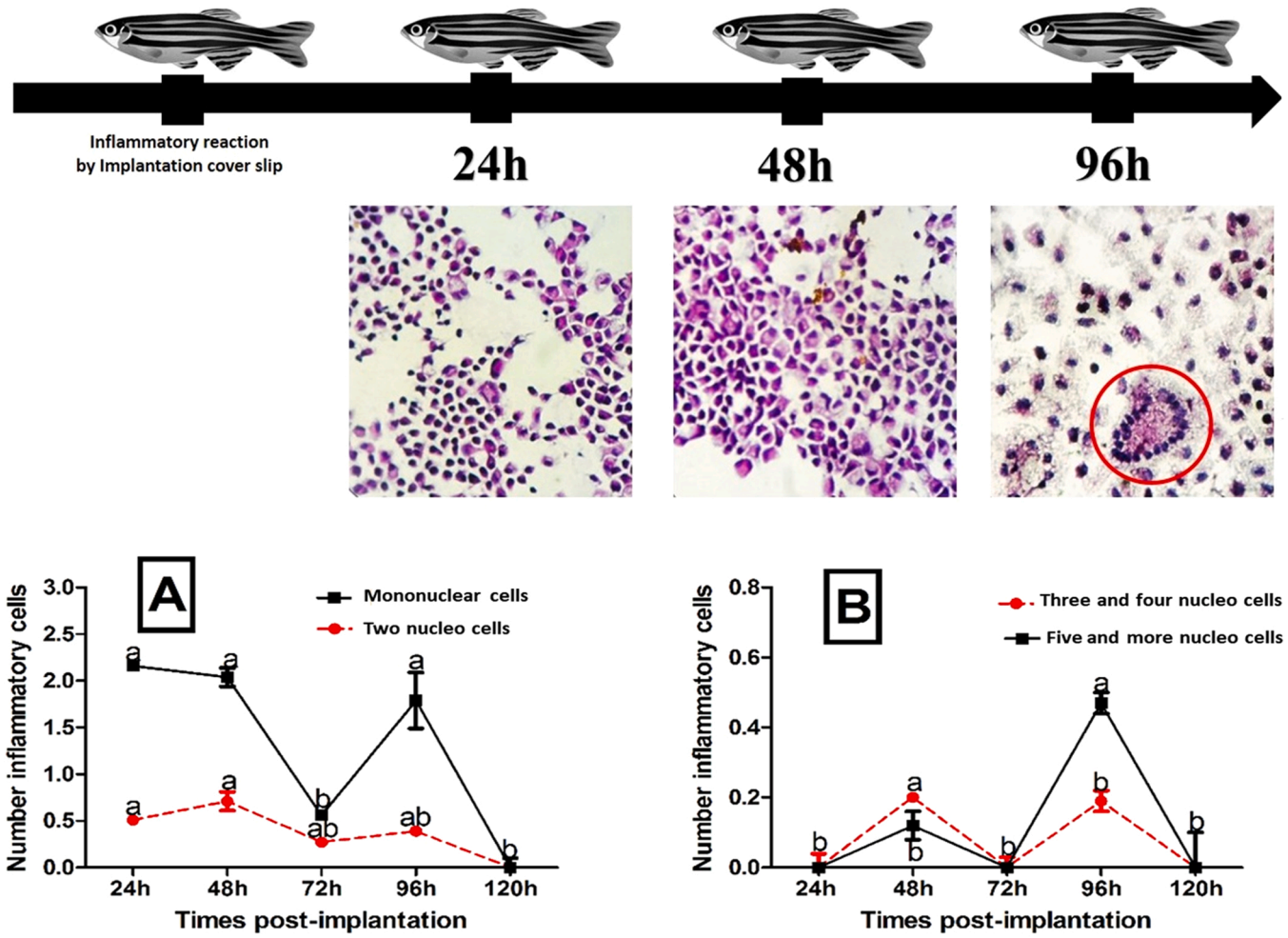

Fig. 10. Mean values (± SE) transformed into (Log x + 1) for total and differential counts of macrophages fixed and polykarions on the implanted glass coverslip in *Danio rerio* at different times. The analysis of variance is represented by lowercase letters for comparison between treatments and different letters indicate a significant difference by the *t*-test ($p < 0.05$). Photomicrograph of macrophages, giant cells, and Langhans-type multinucleated giant cell (LGC) observed under a 400x optical microscope and stained with Hematoxylin & Eosin.

hours, falling within 3 h and returning within 4 h. This first "wave" may be the number of macrophages activated, as suggested earlier, to help signal inflammation. The second "wave" would represent the activity of macrophages during tissue repair. This confirms previous data demonstrating that an increase in NAG is part of the inflammatory process, and our results are in agreement with those reported in the literature [28, 29].

Myeloperoxidase (MPO) is a cationic enzyme composed of two identical dimers connected by a bisulfite bridge, with functionally identical heme groups. It is predominantly found in neutrophils, representing more than 5% of the cell's total protein content. It is released from neutrophil azurophil granules, by different agonists, contributing to the body's innate immune response to infections [30]. MPO catalyzes H_2O_2 formed during oxidative metabolism, as well as chloride ions (Cl^-) to generate hypochlorous acid (HOCl), a more potent cytotoxic oxidant. This enzyme also catalyzes the formation of hypothiocyanate, oxidizes phenols and anilines. This is an important defense mechanism.

However, this substance also promotes oxidative damage to the host tissue, enzyme inactivation, protein crosslinking, amino acid oxidation and, consequently, causes tissue damage at sites of inflammation [30, 31]. MPO activity is related to several pathological conditions associated with neutrophil-mediated inflammation, such as atherosclerosis, rheumatoid arthritis, asthma, cancer, endothelial dysfunction, coronary artery disease, and inflammatory bowel disease [30,31]. Injection of Cg resulted in a concentration-dependent increase in MPO enzyme levels. It was observed an increase in MPO activity 1 h after administration of the treatments, decreasing slightly in the second hour and rising again in the third hour, decreasing immediately thereafter. The MPO activity of animals that received Cg at a concentration of 3.5% was significantly increased at all times compared to the group that received vehicle, and at a concentration of 1.75%, a significant increase was observed only in the first hour. This shows that the effects of the 3.5% concentration are more intense, triggering a more pronounced inflammation, which can be observed and corroborated by the results with the Neubauer chamber experiment. As neutrophils are one of the first groups of defense cells to migrate to the inflamed site, this finding is in agreement with what has been reported in the literature [32].

Subsequently, the histological observations of the images that received Cg in different concentrations showed a worsening of the morphology of the organs, in addition to intense changes evaluated morphometrically. These findings are similar to those described by Prata et al. [7] in zebrafish.

The alterations observed with the use of Cg, such as cell dormancy, cytoplasmic vacuolization, and nuclear displacement in the liver. According to Gayão et al. [33], the displacement of the nucleus to the periphery is an indication that the cell has altered metabolic activity. Numbness of hepatocytes and vacuolization within the cytoplasm resulted in obliteration of hepatic vessels, nuclear displacement, and decreased eosinophilia. Cytoplasmic vacuolization indicates the existence of regions with a probable concentration of glycogen and lipids, or

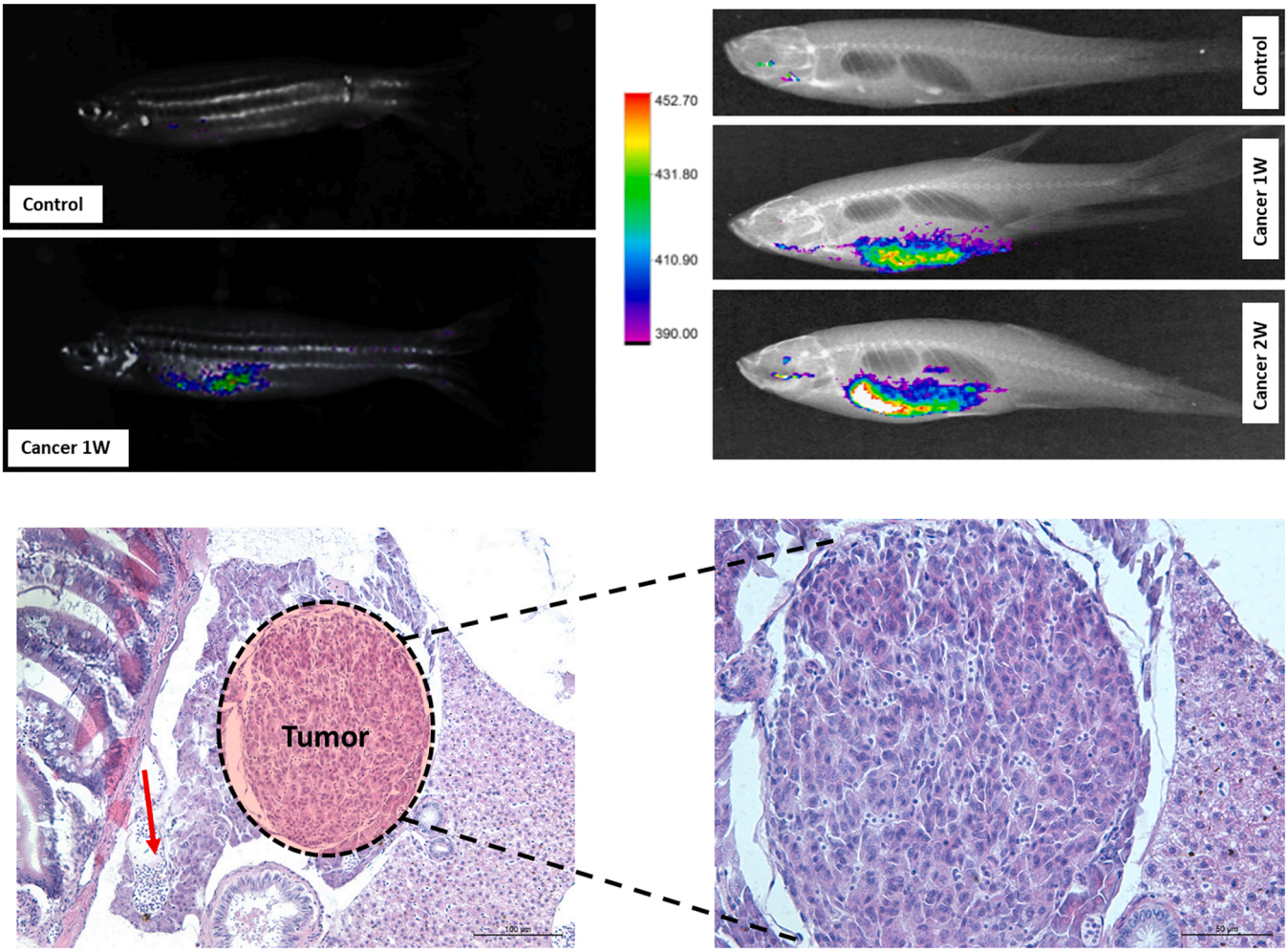

Fig. 11. Xenotransplant of the breast cancer cells (MDA-MB-231) GFP positives and injected into the celomic cavity of the fish (20 μL containing 2000 cells). Xenotransplantation of MDA-MB-231. Fluorescence area measurements demonstrated tumor cells.

the association of toxic agents with intracytoplasmic lipids. Lipid accumulation and decreased glycogen can impair the metabolic activities of hepatocytes and trigger hepatotoxicity [33]. Fish liver is susceptible to chemicals due to slow blood flow relative to the cardiac output. In fact, the biliary excretion of fish is about 50 times slower than that of mammals, making the elimination of toxic products more time-consuming. Toxic substances such as Cg, which reach the liver through the bloodstream, exert their effects on hepatocytes for a longer period than in mammals, directly modifying their morphology and physiological functions [34]. Due to the aggressive condition, leukocyte infiltrates were observed in vessels and tissues, which, according to the literature, is characteristic of an inflammatory process [34].

The mesentery is a fan-shaped organ composed of dense connective tissue, blood and lymph vessels, adipose tissue, and nerves. It helps support the intestine in the abdominal cavity [35]. It is common in fish for the pancreas to be very close to the liver and, in the case of zebrafish, in the mesentery [35]. With the use of Cg, a greater number of mononuclear cells in the connective tissue was observed. It is reported in the literature that mesenteric lymph nodes regulate the migration of leukocytes such as B, T, NK (natural killer) and dendritic cells close to the intestinal mucosa through stimuli, although these mechanisms have not yet been fully elucidated [35]. This could be a hypothesis to justify the increase in mononuclear cells with the injection of the phlogogenic agent Cg. Consistent with the results obtained in the count of inflammatory cells in the Neubauer chamber, when the peak of action was found 4 h after inflammatory stimulation, there was at this period a leukocyte increases as well as significant lesion in the organs of the coelom cavity, dose dependent.

In experiment II, we observed a decrease in circulating leukocytes. These results in zebrafish are different from those observed in other teleosts submitted to this same experimental assay (aerocystitis), as both pacu (*Piaractus mesopotamicus*) and Nile tilapia (*Oreochromis niloticus*) that showed a peak cell accumulation in the inflamed focus within 24 h [23,24]. In the inflammatory reaction of mammals and teleost fish, large amounts of macrophages migrate to the inflamed focus later, and these cells are the object of chronic inflammatory processes studies such as foreign body and granulomatous inflammation [23,36].

In acute aerocystitis, it is possible to detect real-time leukocyte recruitment at the inflammatory site after bacterial infection, with a significant increase in leukocytes and thrombocytes in the exudate. Likewise, circulating leukocytes and thrombocytes had the lowest counts 18 h after challenge, corroborating the findings of the exudate which, in this period, had the highest values, suggesting the occurrence of diapedesis and cell migration to the inflamed focus. Reque et al. [21] and Claudiano et al. [22] found similar results in tilapia and pacus, respectively, clearly demonstrating the importance of thrombocytes in the initial phase of the inflammatory response. According to these authors, unlike platelets in mammals, thrombocytes from teleost fishes, in addition to their activity in the blood coagulation process, play an important role in innate immunity. Despite the controversy in the literature, some authors believe that the thrombocytes of teleost fish even have phagocytic capacity [37], although in the most acute phase

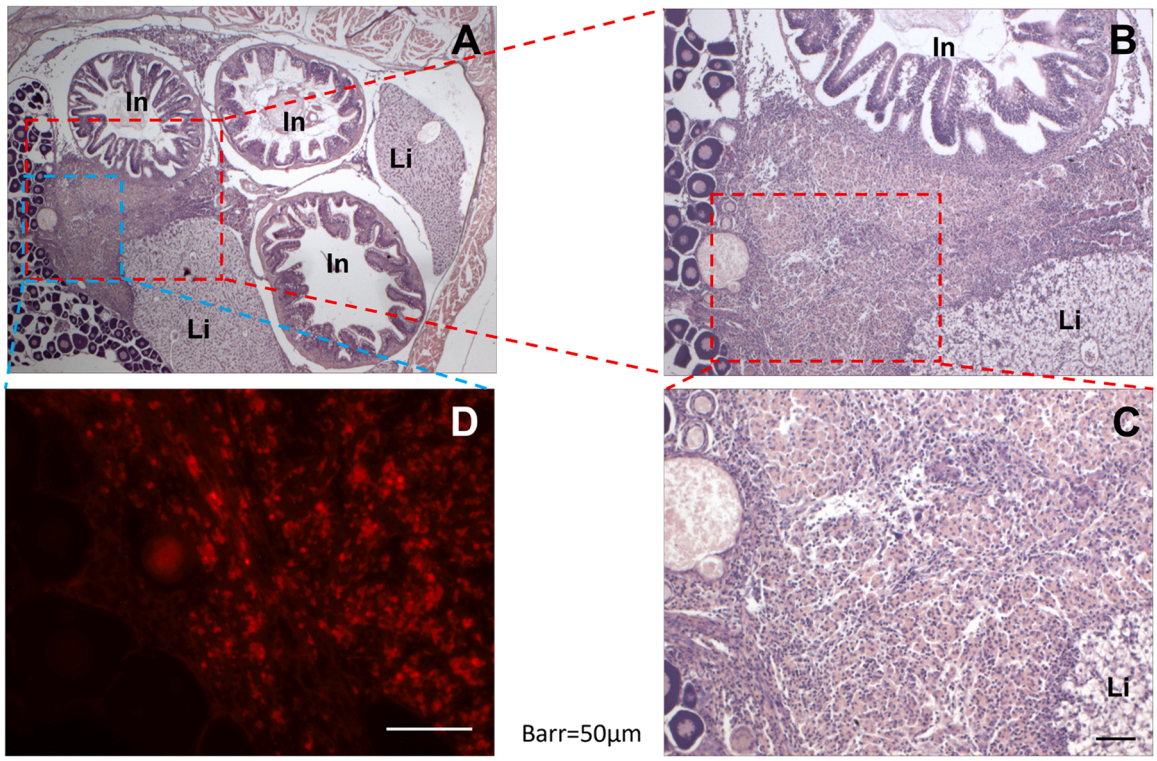

Fig. 12. Light microscopy of H&E-stained zebrafish histological sections. In A, B, C and D, we observe at different magnifications, a cell mass (highlighted in red and blue) with typical characteristics of tumor cells (14 days). In D, at higher magnification, we observe that the mass of cells with tumor characteristics show red fluorescence from the Cell Mask. The xenograft was performed with human breast cancer cells (MGSO-3) labbed by Cell Mask. Sp – spleen, Li – liver, In – intestine, Pa – pancreas.

there was an increase in the relative percentage values of neutrophils and these values were decreasing with the evolution of the inflammatory process. These granulocytes play an important role in acute inflammation [38,39].

Neutrophils are the earliest present leukocyte cells in the injured sites [3,40]. Thus, a high concentration of granulocytic cells represents a transition from its acute phase to a chronification of the inflammatory process.

In experiment III, the presence of a foreign body, in this case a round glass coverslips implanted inside the coelomic cavity, causes macrophages, besides being involved in normal healing, be also responsible to the recognition of foreign surfaces [41]. Coverslip implantation in laboratory animals causes multinucleated giant cells by the fusion of the cell membranes of macrophages derived from monocytes originated in the bloodstream [42]. The implantation of glass coverslips in the subcutaneous tissue or in the peritoneal cavity of rodents became a classic model for studying foreign body inflammation, as macrophages adhere to glass coverslips, even allowing the observation of giant cell formation [43]. In the early 2000 s, this model was successfully adapted to fish by our research group [44,45], since fish macrophages also attach to coverslips, allowing us to assess in vivo the kinetics of cellular accumulation, as well as the formation of foreing body giant cells (FBGCs).

Studies of chronic inflammation during foreign body reactions describe the presence of macrophages and formation of multinucleated giant cells at the interface of an implanted medical device, prostheses and biomaterials (Anderson et al., 2008). In human medicine, this defense response can impact the biocompatibility of implanted devices in tissue engineering and regenerative medicine, needing to clearly establish the pathophysiological mechanisms, which depend on the nature of the implanted biomaterials [41].

McNally and Anderson [46] demonstrated the formation of giant cells by the fusion of macrophages derived from human monocytes after induction with IL-4 and IL-13. In subsequent studies, these authors found that macrophage fusion required mannose receptors (MR) that are highly stimulated by IL-4, as well as the participation of the macrophage endoplasmic reticulum during the cell fusion process, after approximation of these structures to the mannose receptors. Such coupling mechanism presents characteristics similar to those observed in the phagocytosis process [47,48]. According to McNally and Anderson [49], Langhans giant cells (LGC) with circular or semi-circular nuclei arrangement are induced by IFN-γ in the presence of a macrophage maturation factor, such as GM-CSF, M -CSF or IL-3. The antioxidant vitamin E (90% α-tocopherol) induced macrophage fusion and increases IL-4-induced FBGC formation [49]. Similar responses were observed in fish, Belo et al. [50] demonstrated increase in macrophage accumulation and giant cell formation in pacus supplemented with vitamin E.

As observed in mammals, fish showed the same kinetics of macrophage accumulation and cell fusion to form multinucleated cells. In the initial phase of the process, few macrophages attach to the coverslip, with the course of inflammation the accumulation increases and starts the formation of multinucleated cells, which become giants in later phases. In this experimental trial carried out for the first time in zebrafish, it was possible to observe the same kinetics os cell accumulation on the glass coverslip, but it is noteworthy that the course of the inflammatory process was shorter and resulted in the formation of FBGC and Langhans Giant Cells (LGC) within 96 h (4 days) when compared to 8 days observed in tilapia (*Oreochromis niloticus*) [24,51,52] and 15 days in pacus (*Piaractus mesopotamicus*) [44,45,50]. A hypothesis to justify such findings assumes that these fish taxonomically belong to distinct families, and they are on different phylogenetic scales.

In zebrafish, the absence of macrophages observed in the last period can be explained by the high healing stimulus found at the coverslip implant site, causing the influx of neutrophils and macrophages to this region to increase the demand for oxygen, with a consequent increase in the concentrations of lactic acid and pH drop. This combination of hypoxia, low pH and high concentrations of lactic acid activates the

synthesis of an important stimulator of extracellular matrix such as TGF-α by macrophages and fibroblast proliferation [52]. These findings suggest that the implant site may have influenced the progression of the foreign body response as well as the beginning of a healing response. This fact can be seen in the large amount of fibrin present in the 120 h cover slips, making cell quantification impossible.

The rate of macrophage migration to the implanted glass coverslip depends on the nature of the inflammatory reaction and the connective tissue surrounding it. As demonstrated by [43], the inoculation of live BCG (Bacille Calmette-Guerin, Moreaux strain) at the coverslip implant site causes a drastic reduction in the formation of giant cells, reduction in the number of nuclei/giant cell and blockade the Langhans giant cell formation. This phenomenon can be explained by the induction of the inflammatory process caused by live BCG being of high turnover. The opposite occurs with the inoculation of carrageenan, as this substance induces the formation of granuloma with low renewal. Studies performed by our research group described and characterized the kinect of cellular accumulation, as well as cellular components during the evolution of chronic granulomatous inflammation in the teleost fish pacus (*P. mesopotamicus*) induced by BCG, revealing with the use of cell markers S-100, iNOS and cytokeratin that fish granuloma presents the same cell organization observed in mammals (Manrique et al., 2015; 2017).

Exploiting multiple pharmacological inhibitors, [49] studied the participation of phospholipase A2, cyclooxygenase, or lipoxygenase in the mechanism of vacuolar-type ATPase, microtubules and the endoplasmic reticulum (ER) in macrophage fusion, and they confirmed the calcium-independent phospholipase A2 (iPLA2) expression in macrophages/FBGCs. In the teleost fish pacu, the glucocorticoid effect exerted by high circulating cortisol levels resulted in a significant decrease in macrophage accumulation on glass coverslips, as well as in the formation of FBGCs [45,50], and the treatment with dexamethasone demonstrated the same suppressive effect in tilapia [54]. Our research group has been studying the participation of zafirlukast (cysteinyl leukotriene receptor antagonist) and celecoxib (cyclooxygenase-2 inhibitor) in the formation of FBGCs during a foreign body reaction in fish. Preliminary results demonstrate the participation of both drugs in the kinetics of cell accumulation and formation of multinucleated cells (unpublished data). The treatment with cyclophosphamide modulated acute phase proteins and suppressed macrophage accumulation, as well as polykarion formation on glass coverslips during foreign body reaction in the teleost fish tilapia [24]. On the other hand, tilapia treated with levamisole presented increase in the macrophage accumulation and giant cell formation on the glass coverslips [54].

The results observed in this study with zebrafish are very promising, and we believe that significant progress can be made using fish model in determining macrophage fusion factors, signaling pathways, adhesion receptors/proteins, and fusion mechanisms for FBGC formation. Thus, becoming an important alternative tool for studying the foreign body reaction.

In Experiment IV, the use of zebrafish provides a precision to assess the inflammatory response that is of utmost importance in oncology both for evaluating the effectiveness of a treatment and for recognizing the specific clinical, genetic, and molecular inflammatory characteristics of each patient. It provides some advantages such as non-invasive imaging, transgenesis and high-throughput mutagenic assays [54,55].

The zebrafish response to xenotransplantation allows experiments to be of low cost, small size, and because of embryo transparency and rapid external development makes studies completed in days to weeks rather than weeks to months, as is often the case with mammal models [16,44,46,57,58].

In this context, the zebrafish has shown several advantages over other species, such as rodents or provide additional information when used as a model for cancer studies. Interestingly, each fish became a tiny AVATAR model of a patient's cancer [58]. Similar cancer avatars have been created with mice, but the fish approach may be faster and cheaper, making it accessible to more patients. Zebrafish may have a unique niche in cancer treatment. We believe that the use of zebrafish can improve advances in cancer treatment in humans and that Zebrafish can be used in the near future to study new therapies in cancer treatment.

Our four experimental designs presented with zebrafish demonstrate the robustness and versatility of this biomodel to study acute and chronic inflammation. According to Strange [59], zebrafish represents a powerful tool for drug discovery, as they provide particularly unique opportunities for identifying targets and leads discovery of drug candidates. Thus, drug discovery guided by the phenotype in the context of a whole organism can be used to discover compounds that modify the phenotype of the disease, regardless of the specific molecular target. It is noteworthy that the development of many drugs in use today was guided by the phenotype in whole organisms [4]. As an example of the enormous potential of zebrafish in drug development, 16,320 compounds were screened in 16 weeks, around 1000 of compounds per week, in embryos crb mutant which presented increased number of mitotic cells and high rate of cancer [60]. Zanandrea et al. [61] in a comprehensive and complete review strengthen that the Zebrafish models of inflammation and nociception are responsive to treatment with classical steroidal and nonsteroidal anti-inflammatory drugs (NSAIDs) such as aspirin, emphasizing the applicability and the benefits of this organism in inflammation research. A review by Xie et al. [62] shows a very useful table of existing or clinically approved drugs (drug repositioning) that were screened for their ability of suppressing neutrophil recruitment in the zebrafish tail wounding assay. Natural products are also a rich source for drug discovery such as extracts from the medicinal herb ginseng (Panax ginseng) that have been shown to have an inhibitory effect on the infiltration of leukocytes [63]. In addition the results of Prata et al. [7] shows that the peltatoside extracted from a medicinal plant had anti-inflammatory effects both in rodents and zebrafish.

All models (including mammals, non-mammals, cell and tissue cultures, and in vitro assays) have strengths and weaknesses for understanding human disease and drug discovery. An interdisciplinary approach involving different models can improve the understanding of a disease, its therapeutic targets, mechanisms of action and toxicity, reducing the probability of failure and minimizing the high costs for the development of new drugs [59].

4. Conclusion

In addition to the advantages of presenting low production cost, high prolificity and transparent embryos, zebrafish (Danio rerio) proved to be an excellent experimental model for studies of acute and chronic inflammation, allowing the evaluation of edema formation, accumulation of inflammatory cells in the exudate, mediators, signaling pathways, gene expression and production of proteins associated with an inflammatory reaction. Our studies demonstrated the versatility of fish models to investigate the inflammatory response and its pathophysiology, essential tools for the successful development of studies to discover innovative pharmacological strategies.

5. Material and methods

5.1. Zebrafish and conditioning

350 adult zebrafish ($\geq$ 6 months), male and female, with an average weight of 1.0 g $\pm$ 0.29 and from the same spawn were used. To this end, the animals were randomly distributed in 4 trials (I-phlogogen, II - bacteria, III- chronic and IV cancer) and allocated in 35 aquariums ($n = 10$), with a capacity of 5 L of water each, supplied with running water devoid of chlorine and belonging to the creation system of the Pharmacology Laboratory, following the international maintenance standards established by Westerfield [64]. The animals were kept in a system with artificial aeration, with a water flow of 1 L min^{-1}, controlled

temperature of 27 ºC (12 h light:12 h dark photoperiod) and equipped with an ultraviolet lamp. After being transported to the aquariums, the fish were acclimated for 15 days so that the plasmatic concentration of cortisol and osmolarity returned to basal levels. In the first three days of acclimatization, the animals were bathed in a NaCl solution at a concentration of 6.0 g L^{-1}. The fish received pelleted commercial diet (32% crude protein), twice a day, in the morning (8:00 am) and in the afternoon (6:00 pm), corresponding to 3% of the aquarium biomass. The water quality remained within the parameters suitable for the comfort of the species, according to Westerfield (2007), (OD = 6.0 ± 0.123 mgL^{-1}: pH = 7.2 ± 0.78 and electrical conductivity = 110.10 ± 10.30 μS cm^{-1}).

5.2. Anesthesia of fish

Zebrafish were anesthetized by immersion in an aqueous solution of benzocaine at a ratio of 1:10,000 for the administration of inoculum and cover slip implantation and 1:500 at the time of euthanasia. Initially, benzocaine was diluted in 92.8º alcohol (0.1 g/mL), completing the volume to 1 L.

5.3. Acute inflammation with carrageenan assay

5.3.1. Experimental procedure

208 male and female fish with an average weight of 1.0 g All testing procedures were in accordance with the general rules and regulations imposed by the "Ethics Committee in Animal Experimentation at the Federal University of Minas Gerais", approved in 02/10/2017 (Protocol number 248/2017). Carrageenan (Cg) λ type IV was purchased from Sigma (USA) and sterile aqueous solution of sodium chloride (NaCl) 0.9% (sterile saline solution) at concentrations of 0.875%, 1.75% and 3.5%(v/v) was prepared in the laboratory. Drugs will be administered intracelomatic from zebrafish in a volume of 20 μL for all drugs, a method adapted from Huang et al. (2014) and Ekambaram et al. (2017) using an Ultra-Fine ™ BD syringes (Becton, Dickinson and Company), with 300 μL capacity, 6 mm (5/16 ") needle length and 0.25 mm (31 G) caliber.

5.3.2. Experimental design

The animals were distributed in 4 aquariums, randomly divided into four treatments, which were administered: vehicle (sterile saline, control group), Cg at concentration 0.875% (v / v), Cg 1.75% / v) and Cg 3.5% (v / v), with Cg being the inducer of inflammation. After the treatments were injected, the animals were euthanized every hour: 1, 2, 3, 4, 5 and 6 h. Each treatment contained 24 animals, and for each hour, 4 animals were used to perform washing in the coelomic cavity, performing a time-effect curve FOR A Neubauer's chamber. That is, for these two tests, 96 animals were used. Then, the same experimental design was used for measuring the enzymatic activities of NAG and MPO. For these two tests, a further 96 animals were used, distributed in the same 4 treatments. For the histopathological and morphometric analysis, the animals were divided into the same four treatments previously mentioned, with 4 animals each treatment. The histological slides were performed only at a specific time, which was stipulated after the test in the Neubauer chamber, to demonstrate microleads in the organs only at the leukocyte peak. A total of 16 animals were used for histology and morphometry's tests.

5.3.3. Evaluation of inflammatory exudate in the peritoneal cavity

In order to collect the leukocytes, the animals were euthanized, and two washes were performed in the coelomic cavity of each animal, using 100 μL of phosphate buffered saline solution (PBS) in each wash, containing 0.2% heparin, collected the volume with syringe, transferring it to microtubes, with capacity for 2 mL. The lavage was centrifuged at 1200 rpm for 4 min in a refrigerated centrifuge at 4 °C, the supernatant was discarded, and the cells were resuspended with 200 μL of PBS. Then, a 20 μL aliquot of the coelomate lavage was placed in a 2 mL capacity microtube together with 180 μL of Turk's solution and then a 20 μL aliquot was removed and transferred to a Neubauer chamber for total count of leukocytes under optical microscope in final magnification of 100x. Counting was performed in the four lateral quadrants. The mean of the four counts was calculated and the number of leukocytes found was expressed as cells per well x 104, corresponding to the dilution and depth of the Neubauer chamber. This process was based on the methodology of Ferreira and collaborators [65].

5.3.4. Evaluation of the enzymatic activities of Myeloperoxidase (MPO) and N-Acetylglicosaminidase (NAG)

For the verification of macrophages and neutrophils present in the inflammatory process, MPO and NAG, which are enzymes released by neutrophils and macrophages, respectively, were performed [28]. Each animal was processed whole in a 15 mL capacity falcon tube together with a cytokine extraction buffer (NaCl 23.4 g/L, Tween 20 in 500 μL/L, BSA 5 g/L, PMSF 17 mg/L, benzalkonium chloride 44.8 mg/L, EDTA 372 mg/L, aprotinin 20 μL/L.; 1 mL for each 100 mg sample). They were then centrifuged for 10 min at 4 °C at 10,000 rpm. The supernatant was discarded, and the pellet resuspended using Buffer 1 solution (0.1 M NaCl, 0.02 M Na3PO4 and 0.015 M Na2 EDTA) in a ratio of 1.0 mL / 100 mg of tissue and centrifuged for 10 min at 4 °C at 10,000 rpm. The content of each sample was divided into 2 tubes, one for dosing of MPO activity and one for dosing of NAG activity. Again, centrifugation was carried out for 10 min at 4 °C at 10,000 rpm.

For the evaluation of NAG, the supernatant was removed and the pellet 0.9% saline / Triton x-100 [C14H22O (C2H4O) n] 0.1% resuspended in the ratio of 1 mL per 100 mg of sample. It was centrifuged for 10 min at 4 °C at 3000 rpm, and the supernatant was collected. A 100 μL aliquot of each sample was pipetted into a 96-well plate in duplicate plus 100 μL of citrate / phosphate buffer (0.1 M citric acid and 0.1 M Na2HPO4), two wells containing only the buffer citrate / phosphate, corresponding to white. 100 μL of the substrate p-nitrophenyl-N-acetyl-β-D-glucosaminide (0.767 mg / mL diluted in citrate / phosphate buffer) was added, the plate incubated for 10 min at 37 °C. Then, 100 μL of glycine buffer (0.8 M glycine, 0.8 M NaCl and 0.8 M NaOH) was added and the NAG activity was measured using the Biotek ELX800 plate reader (BioTek Instrument) at 405 nm of absorbance, coupled to Gen 5 software (BioTekInstrument), for data analysis. The mean of the values obtained from each duplicate for the dosage of enzyme activity was used. Values were expressed as optical density per gram of proteins (dO/g).

For determination of MPO activity, the supernatant was discarded, and the remaining precipitate was resuspended with Buffer 2 (0.05 M Na3PO4 and 0.5% w/v HETAB) in the ratio of 1 mL per 100 mg. The samples were homogenized, frozen in liquid nitrogen and thawed in water at room temperature, repeating this process 3 times for each sample. It was centrifuged for 15 min at 4 °C at 10,000 rpm and, consequently, the supernatant was collected. 25 μL of each sample was aliquoted into a 96-well plate, in duplicate plus 25 μL of Buffer 2 in each well, two wells containing only Buffer 2, corresponding to white. 25 μL of the 3,3 ', 5,5'-tetramethylbenzidine substrate (1.6 mM TMB, diluted in dimethyl sulfoxide) was added and incubated for 5 min at 37 °C. 100 μL H2O2 (0.002% in buffer 2) was added and incubated again for 5 min at 37 °C. 100 μL of H2SO4 (1 M) was added and the MPO activity was determined using the same plate reader used for dosing NAG, with reading at 450 nm of absorbance, coupled to Gen 5 software (BioTekInstrument), for data analysis. The mean of the values obtained from each duplicate for the enzyme activity dosage was used, being expressed in optical density / mg of proteins (dO / mg). The methodology of Bradley et al. [66] was used.

5.3.5. Histopathological study

To investigate the histopathological changes, the animals were fully fixed in 10% buffered formalin for 24 h. After that period, they were cut

Table 3
Gene submitted to PCR and sequence access in NCBI GenBank.

Gene	rDNA PCR amplificaton		BLAST Details			
			Organism	N° Gen Bank	Query	Max InD
16 S rRNA	Forward primer Reverse primer	AGA GTT TGA TCC TGG CTC AG GGT TAC CTT GTT ACG ACT T	*Aeromonas hydrophila*	JN559379	1688	100%

transversally, placed inside histological cassettes for successive dehydration in ethanol solutions with increasing concentrations (from 70% to 100%) and clarified with xylol baths. Thereafter the animals were embedded in paraffin and sections of 6 μm thick were made using a model 820 (American optical company) rotary microtome, placed on histological slides covered by a layer of albumin. The sections were dewaxed in xylol and rehydrated with decreasing concentrations of ethanol solutions (100–70%), stained with hematoxylin followed by eosin. Subsequently the cuts were dehydrated, diaphanized and the blades assembled for microscopic analysis. This methodology was described by Luna et al. [67], and the liver, intestine and mesentery of the animals were evaluated. The slides were recorded in a 40x objective Olympus model BX51 (Olympus Corporation) microscope coupled to a 2-times projected Q Color 3 Olympus model U-PMTVC (Olympus Corporation). The program used for photographic records was the QCapture (Q Imaging) image analysis program. Then, the images obtained were treated for adjustment of contrast, brightness, and focus, as well as mounted on planks and subtitled using the program Adobe Photoshop CC 2017.

5.3.6. Morphometrical study

The histology slides prepared in the previous step were used to evaluate histomorphological variables of the liver, intestine, and mesentery. Nikon Eclipse E200 (Nikon) light microscopy was used with 100 mm graticule, with 100 fields, coupled to a 10 x eyepiece, with a 40 x objective lens. The liver was evaluated qualitatively by the level of hepatocyte numbness and the level of the cellular infiltrate, being considered the frequency of these parameters as: absent, when no such changes were observed; present, when observed at low frequency; and extreme, when it was predominant over organ morphology. For the mesentery, the percentage of fields containing morphological changes was evaluated: in the intestine, the percentage of fields with epithelial displacement of the villi and the percentage of fields with goblet cells present. In the mesentery was the percentage of fields that contained present infiltrated leukocyte cells. The results were expressed as a percentage in which we analyzed the minimum of 100 fields per animal of each treatment. This methodology was based on the article by Kato et al. [56] and adapted for the organs studied.

5.3.7. Immunohistochemical evaluation

Immunohistochemistry (IHC) was performed according to Eto et al. [68]. After tissue sections, groups of samples were deparaffinized and hydrated, antigen recovery was performed under moist heat with citrate buffer (pH 6.0) for 10 min. Then endogenous peroxidase and nonspecific sites were blocked for 1 h. Primary and secondary antibody added according to the manufacturer's instructions and carried out in a humid chamber at room temperature (28 °C). After incubating the tissue samples with the appropriate antibodies, the IHC sample was washed and incubated with the substrate diaminobenzidine (DAB, Sigma-Aldrich, St. Louis, USA) was mounted and recorded using the same microscope (Olympus BX56 series, Olympus Life Science, Center Valley, PA, USA). Image Analysis: Digital images of five photomicrographs per fish (five fish, n = 5) were captured with a digital camera (Olympus BX56 series, Olympus Life Science, Center Valley, PA, USA). The IHC images used were stained with DAB and hematoxylin. Cells positive for MHC class II cells, IL-1β, TNF-α + and iNOS + were quantified using ImageJ.

5.3.8. Real-time quantitative PCR (qPCR) analysis

For quantitative real-time PCR (qPCR) analyses, RNA samples from all abdominal organs collected at specific time points 1 and 5 h after induction were isolated with Trizon (Sigma). cDNA was obtained using qScript cDNA Supermix (Quanta BioSciences). qPCR was performed by the system according to the manufacturer's instructions. Each sample was tested in duplicate. For each independent experiment, the expression of elongation factor 1-α (ef1a) was scored for each population. The signals detected for each transcript were normalized to beta actin, and the data were analyzed by the ΔΔCt method according to the protocol recommended by the manufacturer (Stratagene). Primers are listed in the Supplemental Materials Table.

5.4. Experimental design for bacteria infection

In the aerocystitis model, fish (n = 60) were randomly distributed by drawing into 6 aquariums of 100 L containing 10 animals each. To this end, zebrafish were inoculated with A. hydrophila in the swim bladder. The bacterial isolate was obtained from naturally infected fish, showing lesions compatible with aeromonosis. To confirm the species, DNA extraction and polymerase chain reaction were performed to amplify the 16S rDNA gene with subsequent sequencing. The sequences obtained were visualized and manipulated in the Sequencer 5.0 program (Gene Codes Corporation), Center for Biological Resources and Genomic Biology – Crebio (UNESP Jaboticabal, SP, Table 3). With the BLASTn tool, the fragment was compared with the sequences deposited in GenBank. The sequencing result confirmed the Aeromonas hydrophila species. With the fish anesthetized, 20 μL of *A. hydrophila* inoculum was injected according to the recommendations of [20] at a concentration of 3 × 109 CFU/mL in the swim bladder.

5.4.1. Leukocyte and thrombocyte counts

At the pre-established times of six, 12, 18, 24, 36 and 48 HPI, blood aliquots were collected in capillaries containing 10 μL of 5000 IU heparin, in the caudal vessel after tail transection. The determination of the global white cell count was carried out in a Neubauer chamber, using the solution of Natt and Herrick with a 1:100 diluent. Differential leukocyte counts were performed on blood smears with a count of 200 cells after prior staining of the stents with May-Grünwald-Giensa-Wrigth [34].

5.4.2. Evaluation of induced exudate in the swim bladder

For the evaluation of total cell accumulation, at the end of the pre-established times of six, 12, 18, 24, 36 and 48 h after the administration of the Aeromonas hydrophila inoculum in the swim bladder, 10 fish per period were dissected by one cut longitudinal ventral from anus to operculum: another from the anus to the head following the lateral line and a third passing through the pectoral fin giving access to the swim bladder. Then, it was carefully washed with 20 μL of ice-cold PBS solution containing 0.09% EDTA. The same injected volume was collected with the aid of a single-channel micropipette (10–100 μL) and transferred to eppendorf kept on ice. An aliquot of this volume was transferred to a Neubauer chamber for counting the total inflammatory cells under light microscopy, stained using the method of Reque et al. [21]. For the differential count of thrombocytes, lymphocytes, macrophages and granulocytes, a drop of this exudate was placed on a histological slide. After homogenization, the exudate was extended and the slide was allowed to dry at room temperature for subsequent fixation with

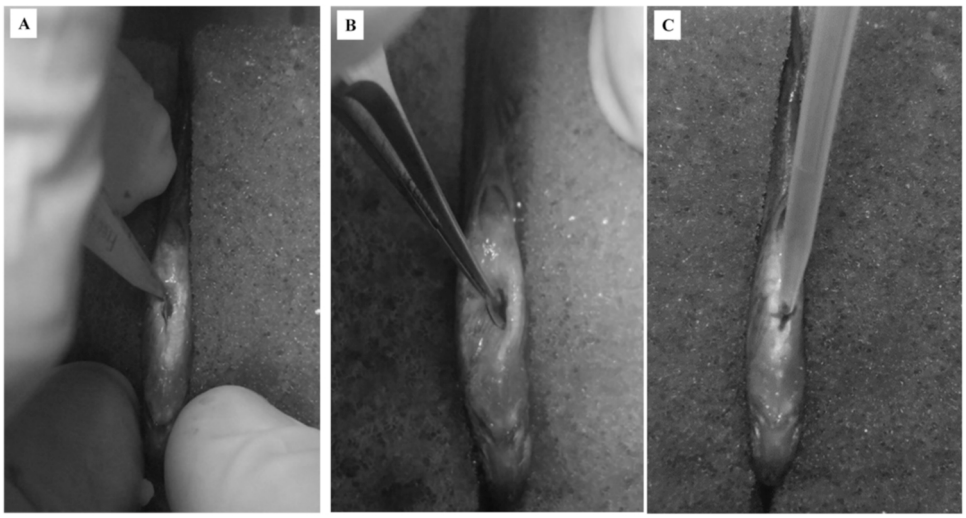

Fig. 13. (A) Incision to give access to the coelomic cavity (B) Coverslip implant (C) Closure of the cavity with Cyanoacrylate.

May-Grunwald-Giemsa-Wrigth dye [21] and counting in light microscopy of up to 200 cells, among the different types accumulated in the inflammatory focus.

5.5. Experimental design for foreign body reaction (chronic inflammation with round glass coverslip implantation)

The fish were randomly distributed by drawing into 7 aquariums of 100 L containing 10 animals each. After being anesthetized, they underwent implantation of a 3 mm-diameter round glass coverslip in the coelomic cavity, following the technique described by Belo et al. [43]. With the aid of a scalpel, the scales around the implant were removed and a small incision was made (Fig. 13 A). After opening the cavity, the cover slip was implanted (Fig. 13B). Then, Glubran® GEM S.r.ʟ-Italy Cyanoacrylate was used for closure (Fig. 13 C). Thus, each fish had a cover slip implanted in its coelomic cavity. After the experimental handling, the animals returned to the aquariums with aeration and continuous water flow again and were sampled in five periods: 24, 48, 72, 96 and 120 h after the implantation of the coverslips to evaluate the cell migration response. Then, euthanasia was performed by immersion in benzocaine diluted in water (1:500) and the coverslips were carefully removed and washed with 0.9% saline solution. Then fixed in Bouin's solution for about a minute and stained in hematoxylin-eosin.

5.6. Experimental design for xenotransplant

Female zebrafish (Danio rerio) were kept in aquariums with a capacity of 5 liters, composed of polypropylene and polystyrene devoid of bisphenol. The cells used in the xenotransplantation were MDA-MB breast tumor cells GFP positive and MGSO-3, labeled with 5 μL of Cell-Mask (ThermoFisher) at 10 nmol/L. After labeling, the tumor cells were included in 7 μL of Matrigel (ECM Gel by Engelbreth-Holm-Swarm - Sigma) and injected into the coelomic cavity of zebrafish (20 μL containing 3000 cells) [58]. A total of 50 female fish were randomly allocated into 2 experimental groups (25 animals per group). Tumor development was analyzed at 3 times over 21 days (T7 days, T14 days and T21 days). Images were acquired using Xtreme – Buckan [69]. Color balance has been fixed and adjusted for display levels. For fluorescence imaging, DsRed filters (for CellMask) were selected, and tumor development was assessed at 7, 14 and 21 dpi. The fluorescence area was determined using ImageJ software (National Institutes of Health). After tumor imaging analysis, zebrafish were fixed in 10% formalin after necropsy. For histopathological analysis, 5-μm-thick sections were mounted on slides and stained with Hematoxylin-Eosin (HE) for observation of general cell structures.

5.7. Statistical analysis

Data normality was measured using the Shapiro-Wilk test. Data that were not normal was transformed into log $x + 1$. After analysis of normality, the experimental data were submitted to analysis of variance through a completely randomized design in split plot in time "Split Plot Design", in two factors, using the statistical package of the SAS software. Comparisons of means were measured by the *t*-test at a 5% significance level.

Acknowledgements

The financial support from the Brazilian funding agencies São Paulo Research Foundation (FAPESP, 2013/25971-9, 2018/07098-0 and 2019/19939-1). Minas Gerais Research Foundation (FAPEMIG) - # APQ-02913-17, National Council for Scientific and Technological Development (CNPq- 477816/2013-4 and 301473 / 2016-1 and CNPq 307526/2018-6).

References

[1] R. Medzhitov, Origin and physiological roles of inflammation, Nature 454 (7203) (2008) 428–435. ⟨https://www.nature.com/articles/nature07201⟩.
[2] I. Goeldner, T.L. Skare, I.T. de M. Reason, S.R. da R. Utiyama, Artrite reumatoide: uma visão atual (Outubro), J. Bras. De. Patol. e Med. Lab. Rio De. Jan. 47 (5) (2011) 495–503, https://doi.org/10.1590/S1676-24442011000500002 (Outubro).
[3] S.A. Renshaw, C.A. Loynes, D.M. Trushell, S. Elworthy, P.W. Ingham, M.K. Whyte, A transgenic zebrafish model of neutrophilic inflammation, Blood 108 (13) (2006) 3976–3978, https://doi.org/10.1182/blood-2006-05-024075.
[4] Leonard I. Zon, T.Peterson Randall, In vivo drug discovery in the zebrafish, Nat. Rev. Drug Discov. 4.1 (2005) 35–44. ⟨https://www.nature.com/articles/nrd1606⟩.
[5] G. Forn-Cuní, M. Varela, P. Pereiro, B. Novoa, A. Figueras, Conserved gene regulation during acute inflammation between zebrafish and mammals, Sci. Rep. 7 (1) (2017) 1–9. ⟨https://www.nature.com/articles/srep41905⟩.
[6] T.M. Tsarouchas, D. Wehner, L. Cavone, T. Munir, M. Keatinge, M. Lambertus, C. G. Becker, Dynamic control of proinflammatory cytokines Il-1β and Tnf-α by macrophages in zebrafish spinal cord regeneration. Nature, Communications 9 (1) (2018) 1–17. ⟨https://www.nature.com/articles/s41467-018-07036-w⟩.
[7] M.N.L. Prata, I. Charlie-Silva, J.M.M. Gomes, A. Barra, B.B. Berg, I.R. Paiva, A. C. Perez, Anti-inflammatory and immune properties of the peltatoside, isolated from the leaves of Annona crassiflora Mart., in a new experimental model zebrafish, Fish. Shellfish Immunol. 101 (2020) 234–243, https://doi.org/10.1016/j.fsi.2020.03.044.
[8] S.C. Baraban, M.T. Dinday, G.A. Hortopan, Drug screening in Scn1a zebrafish mutant identifies clemizole as a potential Dravet syndrome treatment, Nat. Commun. 4 (1) (2013) 1–10. ⟨https://www.nature.com/articles/ncomms3410⟩.
[9] I. Charlie-Silva, N.M. Feitosa, J. Gomes, D. Hoyos, C.C. Mattioli, S.F. Eto, D. C. Fernandes, M. Belo, J.O. Silva, A. Barros, J.D. Corrêa Junior, G.B. de Menezes,

H. Fukushima, T. Castro, R.C. Borra, F. Pierezan, N. de Melo, L.F. Fraceto, Potential of mucoadhesive nanocapsules in drug release and toxicology in zebrafish, PLoS One 15 (9) (2020), e0238823, https://doi.org/10.1371/journal.pone.0238823.
[10] I. Charlie-Silva, N.M. Feitosa, H. Fukushima, R.C. Borra, M.A. Foglio, R. Xavier, D. C. de Melo Hoyos, I.M. de Oliveira Sousa, G.G. de Souza, R.L. Bailone, M.A. de Andrade Belo, S. Correia, J. Junior, F. Pierezan, G. Malafaia, Effects of nanocapsules of poly-ε-caprolactone containing artemisinin on zebrafish early-life stages and adults, Sci. Total Environ. 756 (2021), 143851, https://doi.org/10.1016/j.scitotenv.2020.143851.
[11] A.T.B. Guimarães, I. Charlie-Silva, G. Malafaia, Toxic effects of naturally-aged microplastics on zebrafish juveniles: a more realistic approach to plastic pollution in freshwater ecosystems, J. Hazard. Mater. 407 (2021), 124833, https://doi.org/10.1016/j.jhazmat.2020.124833.
[12] J.M. Mendonça-Gomes, A.P. da Costa Araújo, T.M. da Luz, I. Charlie-Silva, H. Braz, R. Jorge, M. Ahmed, R.H. Nóbrega, C. Vogel, G. Malafaia, Environmental impacts of COVID-19 treatment: Toxicological evaluation of azithromycin and hydroxychloroquine in adult zebrafish, Sci. Total Environ. 790 (2021), 148129, https://doi.org/10.1016/j.scitotenv.2021.148129.
[13] Calum A. MacRae, T.Peterson Randall, Zebrafish as tools for drug discovery, Nat. Rev. Drug Discov. 14.10 (2015) 721–731. ⟨https://www.nature.com/articles/nrd4627⟩.
[14] E.E. Patton, L.I. Zon, D.M. Langenau, Zebrafish disease models in drug discovery: from preclinical modelling to clinical trials, Nat. Rev. Drug Discov. (2021) 1–18. ⟨https://www.nature.com/articles/s41573-021-00210-8⟩.
[15] M.A.A. Belo, I. Charlie-Silva, Teleost fish as an experimental model for vaccine development, in: S. Thomas (Ed.), Vaccine Design, 66, Springer-Nature, 2014, pp. 1080–1105.
[16] K. Howe, M.D. Clark, C.F. Torroja, J. Torrance, C. Berthelot, M. Muffato, M. Teucke, The zebrafish reference genome sequence and its relationship to the human genome, Nature 496 (7446) (2013) 498–503. ⟨https://www.nature.com/articles/nature12111⟩.
[17] A. Andrade, S.C. Pinto, R.S.D. Oliveira, Animais de laboratório: criação e experimentação, Ed. Fiocruz (2006). ⟨http://books.scielo.org/id/sfwtj⟩.
[18] C.A. Winter, E.A. Risley, G.W. Nuss, Carrageenin-induced edema in hind paw of the rat as an assay for antiinflammatory drugs, Proc. Soc. Exp. Biol. Med. 111 (3) (1962) 544–547, https://doi.org/10.3181/00379727-111-27849.
[19] T. Cunha, W.A. Verri, J.S. Silva, S. Poole, F.Q. Cunha, S.H. Ferreira, A cascade of cytokines mediates mechanical inflammatory hypernociception in mice, Proc. Natl. Acad. Sci. USA 102 (5) (2005) 1755–1760, https://doi.org/10.1073/pnas.0409225102.
[20] I. Charlie-Silva, A. Klein, J.M. Gomes, E.J. Prado, A.C. Moraes, S.F. Eto, M.A. Belo, Acute-phase proteins during inflammatory reaction by bacterial infection: Fish-model, Sci. Rep. 9 (1) (2019) 1–13. ⟨https://www.nature.com/articles/s41598-019-41312-z⟩.
[21] V.R. Reque, J.R.E. de Moraes, M.A. de Andrade Belo, F.R. de Moraes, Inflammation induced by inactivated Aeromonas hydrophila in Nile tilapia fed diets supplemented with Saccharomyces cerevisiae, Aquaculture 300 (1–4) (2010) 37–42, https://doi.org/10.1016/j.aquaculture.2009.12.014.
[22] M.P. de Castro, G.S. Claudiano, N.L. Bortoluzzi, E. Garrido, R.Y. Fujimoto, M.A. A. Belo, F.R. Moraes, Chromium carbochelate dietary supplementation favored the glucocorticoid response during acute inflammation of Piaractus mesopotamicus, Aquaculture 432 (2014) 114–118, https://doi.org/10.1016/j.aquaculture.2014.04.036.
[23] M.A.A. Belo, S.H.C. Schalch, F.R. Moraes, V.E. Soares, A.M.M.B. Otoboni, J.E. R. Moraes, Effect of dietary supplementation with vitamin E and stocking density on macrophage recruitment and giant cell formation in the teleost fish, Piaractus mesopotamicus, J. Comp. Pathol. 133 (2–3) (2005) 146–154, https://doi.org/10.1016/j.jcpa.2005.04.004.
[24] I. Charlie-Silva, G. Conde, J.M.M. Gomes, E.J. da Rosa Prado, D.C. Fernandes, A. C. de Moraes, M.A.A. Belo, Cyclophosphamide modulated the foreign body inflammatory reaction in tilapia (Oreochromis niloticus), Fish. Shellfish Immunol. 107 (2020) 230–237, https://doi.org/10.1016/j.fsi.2020.09.039.
[25] S.P. Ekambaram, S.S. Perumal, S. Pavadai, Anti-inflammatory effect of Naravelia zeylanica DC via suppression of inflammatory mediators in carrageenan-induced abdominal oedema in zebrafish model, Inflammopharmacology 25 (1) (2017) 147–158, https://doi.org/10.1007/s10787-016-0303-2.
[26] R.A.L.P.H. Vinegar, J.F. Truax, J.L. Selph, F.A. Voelker, Pathway of onset, development, and decay of carrageenan pleurisy in the rat, Fed. Proc. 41 (9) (1982) 2588–2595. ⟨https://pubmed.ncbi.nlm.nih.gov/6806127⟩.
[27] Y. Luqmani, L. Temmim, A. Memon, L. Abdulaziz, A. Parkar, M. Ali, H. Baker, M. Motawy, S. Fayaz, Measurement of serum N-acetyl beta glucosaminidase activity in patients with breast cancer, Acta Oncol. 38 (5) (1999) 649–653, https://doi.org/10.1080/028418699431267.
[28] P.J.; Bailey, A.; Sturm, B. Lopez-Ramos, A biochemical study of the cotton pellet granuloma in the rat, Eff. Dexamethasone Indomethacin. Biochem. Pharmacol. 31 (7) (1992) 1213–1218.
[29] T.A. Gheita, A.M.N.E.D. Abd, E. Baky, H.S. Assal, T.M. Farid, I.A. Rasheed, E. H. Thabet, Serum cystatin C, urinary neutrophil gelatinase-associated lipocalin and N-acetyl-beta-D-glucosaminidase in juvenile and adult patients with systemic lupus erythematosus: correlation with clinical manifestations, disease activity and damage, Saudi J. Kidney Dis. Transplant. 26 (3) (2015) 497–506. ⟨https://www.sjkdt.org/text.asp?2015/26/3/497/157336⟩.
[30] R.M. Roman, A.E. Wendland, C.A. Polanczyk, Mieloperoxidase e doença arterial coronariana: da pesquisa à prática clínica. Arquivos Brasileiros de Cardiologia, i. 1. São Paulo. 91 (2008) e12–e19.
[31] P. Guilpain, A. Servettaz, F. Batteux, L. Guillevin, L. Mouthon, Natural and disease associated anti-myeloperoxidase (MPO) autoantibodies, Autoimmun. Rev. 7 (6) (2008) 421–425, https://doi.org/10.1016/j.autrev.2008.03.009.
[32] D. Male, J. Brostoff, D.B. Roth, I. Roitt, Immunology. 7ª edição. Filadelfia, Mosby Elsevier, 2006, pp. 127–144.
[33] A.L.B. Gayão, A. de, H. Buzollo, G.C. Fávero, A.A. e Silva Junior, M.C. Portella, C. da Cruz, D.J. Carneiro, Histologia hepática e produção em tanques-rede de tilápia-do-nilo masculinizada hormonalmente ou não masculinizada, 48, Pesquisa Agropecuária Brasileira, Brasília, 2013, pp. 991–997, https://doi.org/10.37496/rbz4920190032.
[34] C.M.D. Campos, J.R. de Moraes, F.R.D. Moraes, Histopatologia de fígado, rim e baço de Piaractus mesopotamicus, Prochilodus lineatus e Pseudoplatystoma fasciatum parasitados por myxosporídios, capturados no Rio Aquidauana, Mato Grosso do Sul, Brasil, Rev. Bras. De. Parasitol. Veter. 17 (2008) 200–205, https://doi.org/10.1590/S1984-29612008000400006.
[35] J.C. Coffey, D.P. O'Leary, The mesentery: structure, function, and role in disease, Lancet Gastroenterol. Hepatol. 1 (3) (2016) 238–247, https://doi.org/10.1016/S2468-1253(16)30026-7.
[36] W.G. Manrique, S. Claudiano Gda, M.P. de Castro, T.R. Petrillo, M.A. Pereira Figueiredo, M.A. Belo, M.I. Berdeal, J.E. de Moraes, F.R. de Moraes, Expression of cellular components in granulomatous inflammatory response in Piaractus mesopotamicus model, PLoS One 10 (3) (2015), e0121625, https://doi.org/10.1371/journal.pone.0121625.
[37] M. Tavares-Dias, F.R. Moraes, M.L. Martins, Hematological assessment in four Brazilian teleost fish with parasitic infections, collected in feefishing from Franca, São Paulo, Brazil, Bol. do Inst. De. Pesca 34 (2) (2008) 189–196. ⟨https://www.pesca.sp.gov.br/boletim/index.php/bip/article/view/785⟩.
[38] M.A.A. Belo, F.R. de Moraes, L. Yoshida, E.J. da Rosa Prado, J.R.E. de Moraes, V. E. Soares, M.G. da Silva, Deleterious effects of low level of vitamin E and high stocking density on the hematology response of pacus, during chronic inflammatory reaction, Aquaculture 422 (2014) 124–128, https://doi.org/10.1016/j.aquaculture.2013.12.013.
[39] M.A.A. Belo, D.G.F. Souza, V.P. Faria, E.J.R. Prado, F.R. Moraes, E.M. Onaka, Haematological response of curimbas Prochilodus lineatus, naturally infected with Neoechinorhynchus curemai, J. Fish. Biol. 82 (4) (2013) 1403–1410, https://doi.org/10.1111/jfb.12060.
[40] S. De Oliveira, C.C. Reyes-Aldasoro, S. Candel, S.A. Renshaw, V. Mulero, Â. Calado, Cxcl8 (IL-8) mediates neutrophil recruitment and behavior in the zebrafish inflammatory response, J. Immunol. 190 (8) (2013) 4349–4359, https://doi.org/10.4049/jimmunol.1203266.
[41] Z. Sheikh, P.J. Brooks, O. Barzilay, N. Fine, M. Glogauer, Macrophages, foreign body giant cells and their response to implantable biomaterials, Materials 8 (9) (2015) 5671–5701, https://doi.org/10.3390/ma8095269.
[42] T. GILLMAN, L.J. WRIGHT, Probable in vivo origin of multinucleate giant cells from circulating mononuclears, Nature 209 (1966) 263–265. ⟨https://www.nature.com/articles/209263a0⟩.
[43] M. Mariano, W.G. Spector, The formation and properties of macrophage polykaryons (inflammatory giant cells), J. Pathol. 113 (1) (1974) 1–19, https://doi.org/10.1002/path.1711130102.
[44] M.C. PETRIC, et al., Polycarion macrophage formation kinetics in Piaractus mesopotamicus Holmberg, 1887 (Osteichthyes: Characidae), in: Experimental Model, 29, Boletim do Instituto de Pesca, 2003, pp. 95–100.
[45] M.A.D.A. Belo, S.H.C. Schalch, F.R. Moraes, V.E. Soares, A.M.M.B. Otoboni, J.E. R. Moraes, Effect of dietary supplementation with vitamin E and stocking density on macrophage recruitment and giant cell formation in the teleost fish, Piaractus mesopotamicus, J. Comp. Pathol. 133 (2–3) (2005) 146–154, https://doi.org/10.1016/j.jcpa.2005.04.004.
[46] A.K. Mcnally, J.M. Anderson, Interleukin-4 induces foreign body giant cells from human monocytes/macrophages, Am. J. Pathol. 147 (1995) 1487–1499.
[47] A.K. Mcnally, J.M. Anderson, Interleukin-4 induced macrophage fusion is prevented by inhibitors of mannose receptor activity, Am. J. Pathol. 149 (1996) 975–998.
[48] A.K. MCNALLY, J.M. ANDERSON, Multinucleated giant cell formation exhibits features of phagocytosis with participation of the endoplasmic reticulum, Exp. Mol. Pathol. 79 (2005) 126–135.
[49] A.K. MCNALLY, J.M. ANDERSON, Foreign body-type multinucleated giant cell formation is potently induced by α-tocopherol and prevented by the diacylglycerol kinase inhibitor R59022, Am. J. Pathol. 163 (2003) 1147–1156.
[50] M.A.D.A. Belo, J.R.E.D. Moraes, V.E. Soares, M.L. Martins, C.D. Brum, F.R. D. Moraes, Vitamin C and endogenous cortisol in foreign-body inflammatory response in pacus, Pesqui. Agropecuária Bras. 47 (2012) 1015–1021, https://doi.org/10.1590/S0100-204X2012000700019.
[51] R. SAKABE, F. R. de Moraes, M.A. de A. Belo, J.R.E. de Moraes, Kinetics of chronic inflammation in Nile tilapia fed n-3 and n-6 essential fatty acids, Pesqui. Agropecuária Bras. 48 (2013) 313–319.
[52] C.A. Balbino, L.M. Pereira, R. Curi, Mecanismos envolvidos na cicatrização: uma revisão, Rev. Bras. De. Ciências Farm. 41 (2005) 27–51.
[54] T.R. Petrillo, G.S. CLAUDIANO, J.Y. Aguinaga, MANRIQUE, G.Ó.M.E.Z. WILSON, M.P. Castro, M.A.A. BELO, J.R.E. MORAES, F.R. Moraes, Influence of dexamethasone and levamisole on macrophage recruitment, giant cell formation and blood parameters in the tropical fish Piaractus mesopotamicus, Biosci. J. (UFU) 33 (2017) 1015–1027.
[55] R. Fior, V. Póvoa, R.V. Mendes, T. Carvalho, A. Gomes, N. Figueiredo, M. G. Ferreira, Single-cell functional and chemosensitive profiling of combinatorial colorectal therapy in zebrafish xenografts, Proc. Natl. Acad. Sci. USA 114 (39) (2017) E8234–E8243, https://doi.org/10.1073/pnas.1618389114.

[56] C.R. de Almeida, R.V. Mendes, A. Pezzarossa, J. Gago, C. Carvalho, A. Alves, R. Fior, Zebrafish xenografts as a fast screening platform for bevacizumab cancer therapy, Commun. Biol. 3 (1) (2020) 1–13.
[57] V. Póvoa, C.R. de Almeida, M. Maia-Gil, D. Sobral, M. Domingues, M. Martinez-Lopez, R. Fior, Innate immune evasion revealed in a colorectal zebrafish xenograft model, Nat. Commun. 12 (1) (2021) 1–15. ⟨https://www.nature.com/articles/s41467-021-21421-y⟩.
[58] M. Leslie, Zebrafish larvae could help to personalize cancer treatments, Zebra larvae Could Help Pers. Cancer Treat. 357 (2017) 745, https://doi.org/10.1126/science.357.6353.745.
[59] J.M. Mendonça-Gomes, T.M. Valverde, T.M.M. Martins, I. Charlie-Silva, B. N. Padovani, C.M. Fénero, E.M. da Silva, R.Z. Domingues, D.C. Melo-Hoyos, J. D. Corrêa-Junior, N.O.S. Câmara, A.M. Góes, D.A. Gomes, Long-term dexamethasone treatment increases the engraftment efficiency of human breast cancer cells in adult zebrafish, Fish. Shellfish Immunol. Rep. 2 (2021), 100007, https://doi.org/10.1016/j.fsirep.2021.100007.
[60] K. Strange, Drug discovery in fish, flies, and worms, ILAR J. 57 (2) (2016) 133–143.
[61] H.M. Stern, L.I. Zon, Cancer genetics and drug discovery in the zebrafish, Nat. Rev. Cancer 3 (2003) 533–539.
[62] R. Zanandrea, D. Carla, C.D. Bonan, M.M. Campos, Zebrafish as a model for inflammation and drug discovery (doi.org/), Drug Discov. Today 25 (2020) 2201–2211, https://doi.org/10.1016/j.drudis.2020.09.036.
[63] Y.; Xie, A.H. Meijer, M.J.M. Schaaf, Modeling inflammation in zebrafish for the development of anti-inflammatory drugs, Front. Cell Dev. Biol. 8 (2021), 620984, https://doi.org/10.3389/fcell.2020.620984.
[64] M. Sun, M. He, H. Korthout, M. Halima, H.K. Kim, Y. Yan, E. van Wijk, R. van Wijk, C. Guo, M. Wang, Characterization of ginsenoside extracts by delayed luminescence, high-performance liquid chromatography, and bioactivity tests, Photochem. Photobiol. Sci. 18 (2019) 1138–1146, https://doi.org/10.1039/C8PP00533H.
[65] M. Westerfield, The zebrafish book: a guide for the laboratory use of zebrafish (Danio rerio). Institute of Neuroscience, 5th ed., University of Oregon, 2007.
[66] R.G. Ferreira, T.C. Matsui, L.F. Gomides, A.M. Godin, G.B. Menezes, M. de Matos Coelho, A. Klein, Niacin inhibits carrageenan-induced neutrophil migration in mice, Naunyn Schmiede 'S. Arch. Pharmacol. 386 (6) (2013) 533–540, https://doi.org/10.1007/s00210-013-0854-3.
[67] P.J. Bailey, A. Sturm, B. Lopez-Ramos, A biochemical study of the cotton pellet granuloma in the rat: effects of dexamethasone and indomethacin, Biochem. Pharmacol. 31 (7) (1982) 1213–1218, https://doi.org/10.1016/0006-2952(82)90006-5.
[68] L.G. Luna, Manual of histologic staining methods of the Armed Forces Institute of Pathology. 3ª edição. Nova Iorque, McGraw-Hill, 1968.
[69] S.F. Eto, D.C. Fernandes, A.C. Moraes, E.J.R. Prado, A.C. Baldassi, W.G. Manrique, J.M. Pizauro, Validation of IgY for the diagnosis of Streptococcus agalactiae-caused endocarditis and bacterial meningitis in Nile tilapia (Oreochromis niloticus), Fish. Shellfish Immunol. 76 (2018) 153–160, https://doi.org/10.1016/j.fsi.2018.02.048.